國立臺灣大學理學院物理學系

碩士論文

Department of Physics

College of Science

National Taiwan University

Master Thesis

使用約瑟夫森分支放大器的量子測量之研究

Study of Quantum Measurement by a Superconducting

Josephson Bifurcation Amplifier

柯百謙

Bai-Cian Ke

指導教授：管希聖 博士

Advisor: Hsi-Sheng Goan, Ph.D.

中華民國 98 年 7 月

July, 2009

# 誌　謝

氣。在絕望的時候給了我一個希望，讓我開始變得樂觀，真的非常感謝她無私的付出。

要感謝的人很多，掛一漏萬，若有遺漏在此也一併獻上內心最深的謝意。

# 摘　要

　　最近，一種新型的放大器，稱為約瑟夫森分支放大器（JBA），用以測量超導量子位元（qubit），已經被提議和建造出來。JBA 解決了建構在傳統超導 Josephson junction 量子位元測量裝置的散熱問題，此惱人的散熱問題是由此裝置的電壓切換到 normal state 所引起 。本論文旨在模擬使用 JBA 測量量子位元的過程，並提供對理解量子測量問題所必需的相關知識。我們一開始回顧一些基本的超導量子電路元件，並介紹兩種不同類型的量子位元：flux qubit 和 charge qubit。由於 Josephson junction 的非線性電感，JBA 的數學模型可由驅動非線性振盪器所描述，此數學模型被稱為 Duffing 振子。因此，我們著重於量子 Duffing 振子的性質和介紹 JBA 的運作原理 。測量量子位元的過程本身是一個開放量子系統的問題。為了來描述它的行為，我們推導了驅動 Duffing 振子和量子位元系統的縮減密度矩陣的 quantum master equation。我們區分了熱環境和測量裝置對系統的影響，並使用 Floquet formalism 處理時間上的週期性問題。並在最後提出一些 Duffing 振子和量子位元測量的模擬結果。

## ABSTRACT

Recently, a new type of amplifier, called the Josephson bifurcation amplifier (JBA), to read out the state of a superconducting quantum bit (qubit), has been proposed and constructed. This JBA has solved the annoying dissipation problem of voltage switching to the normal state in traditional superconducting Josephson junction based qubit measurement devices. This thesis aims to model the qubit readout process by the JBA, and to provide the essential input toward the understanding of the quantum measurement problem. We first review some basic elements of superconducting quantum circuit, and introduce two different types of qubits: flux qubits and charge qubits. Due to the non-linear inductance of a Josephson junction, the mathematical model of the JBA can be linked to a driven non-linear oscillator, known as the Duffing oscillator. So we focus on the properties of the quantum Duffing oscillator and present the operation principles of the JBA. The qubit readout process is itself an open quantum system problem. To describe its dynamics, we derive the quantum master equation for the reduced density matrix of the combined driven quantum Duffing oscillator and qubit system. We distinguish the influence of the thermal environment on the combined system from that of the measurement device, and use the Floquet formalism to tackle the time-periodical driven problem. Simulation results of the Duffing oscillator and qubit measurement will be presented.

# Contents

# List of Figures

# Chapter 1

# Introduction

The quantum information science has developed for decades. In the beginning, it didn't draw much attention, because no quantum algorithms that had practical use and outperformed their classical counterparts were found. Not only it has great difficulties to realize a quantum computer, but also researchers even thought that the calculating speed of a quantum computer is much slower than the speed of a classical computer. This situation remained until Shor's algorithm [1, 2] and Grover's algorithm [3–5] were proposed. Shor's algorithm makes it possible to efficiently factorize large semi-prime integers and Grover's algorithm enables searches within a large unsorted database. Those two problems are impossible solved or very time-consuming for a classical computer. People recognized a problem difficult for a classical computer to solve may be easy to solve for a quantum computer. Because of those key motivations, people pay more and more attention on the field of quantum information science.

"Is it possible to realize a quantum computer?", many people may ask this question. In fact, it is still a very long distance for people to realize a practical quantum

computer. However, regardless whether a quantum computer can be built ultimately, people will still benefit much on the road to the final goal of implement a quantum computer. Researchers have been trying to find methods to control quantum systems precisely, and to develop controllable quantum systems to construct universal quantum gates [6], which can be used to implement arbitrary unitary operations. Those methods and devices developed may be used in other purposes. Although few-qubit controls and manipulations are still a challenge, it is believed that one day the quantum computer will be realized.

There are three stages in quantum computation : preparation, manipulation, and readout. In this thesis, we focus on the readout process. At the end of quantum-state manipulation, we need to read out the final results. Or even in the middle of manipulation, we read out the qubit's state for the purpose of error correction. Many traditional schemes to read out the states of superconducting Josephson junction qubits, such as the phase qubit, quantronium etc., are involved with the voltage switching of a readout Josephson junction to the dissipative normal state under the direct measurement. A new type of amplifier, the Josephson bifurcaiton amplifier (JBA) [7], to read out the states of a qubit, constructed by I. Siddiqi *et al.* in 2004, has solved the annoying dissipation problem. The mathematical model of the JBA is a driven non-linear oscillator, known as the Duffing oscillator in classical physics [8,9].

This thesis investigates the quantum Duffing oscillator and some basic super-conducting quantum information devices. First we review some basic elements of quantum circuits: Josephson junctions, superconducting Cooper-pair boxes (SCB's), and superconducting quantum interference devices (SQUID's). The property of behaving like a nonlinear inductance makes the Josephson junction play a crucial role
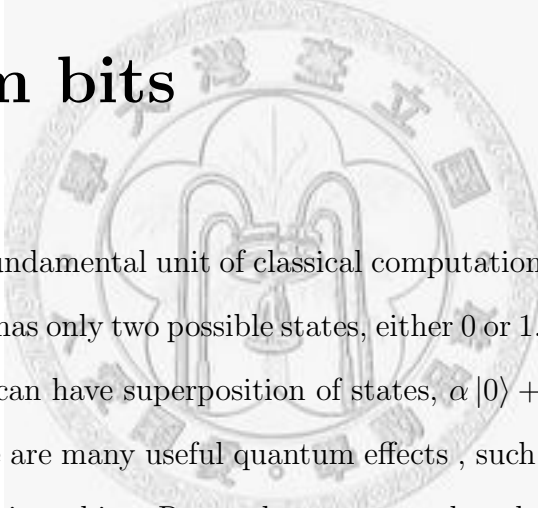
in a quantum circuit. The discrete Cooper-pair number in SCB and the magnetic flux quantum number make, respectively, the SCB and the SQUID ideal candidates as qubits. Then we introduce basic types of quantum bits, flux qubits and charge qubits, and a special kind of qubit in charge-phase regime, called the quantronium. After that, we present an introduction of the working principle of a JBA and how a JBA can be modeled as a driven quantum Duffing oscillation.

Second, we describe a mathematical technique, the Floquet formalism, usually used to deal with time-periodic problems. Analogous to the Bloch theory, the principle of the Floquet formalism is to expanse ,besides the space domain, the time domain function by a time-periodic basis, $e^{in\omega t}$. Next, we introduce the concept of a master equation. In an open system, the Schrödinger equation is no longer sufficient to describe the dynamics of the system of interest. The density matrix and the master equation is thus required. Then, we present the master equation for a driven system, which differ form the ordinary master equation, that is usually in the Lindblad form. There are time-ordering operators inside the time-dependent master equation, which could be very troublesome.

Finally, we present a master equation with Floquet states as a basis. In the Floquet picture, the problem of the time-ordering operators is readily solved. Consequently, the dynamics of the driven quantum Duffing oscillator can be described more easily by using this improved master equation. Then we describe how to use a JBA to measure a qubit, present some numerical results and discuss the dynamical behavior of the combined system of JBA and the measured qubit.

# Chapter 2

# Introduction to superconducting quantum bits

A bit is the most fundamental unit of classical computation and information. A bit in a classic computer has only two possible states, either 0 or 1. Besides $|0\rangle$ or $|1\rangle$, a quantum bit, or qubit, can have superposition of states, $\alpha |0\rangle + \beta |1\rangle$ with $|\alpha|^2 + |\beta|^2 = 1$. Furthermore, there are many useful quantum effects , such as quantized energy levels and entanglement, in qubits. Researchers try to take advantage of quantum effects and hope to ultimately create quantum computers to solve time-consumsing problems or problems which are impossible to be solved in classical computers, such as factoring large numbers and simulating large quantum systems.

A quantum superconducting Josephson-junction circuit may contain a large numbers of energy levels, while for qubit operations only two levels are required. Moreover, these two qubit levels must be well decoupled from the other levels. Typically, that means that a qubit should involve a low-lying pair of levels, well separated from the spectrum of higher levels, and not being close to resonance with any other levels.

There are three stages in quantum computation : preparation, manipulation, and readout. Although any quantum two-state system can be considered as a qubit, to be able to be isolated from other energy levels and environment and to be prepared, manipulated, and read out determine whether it is a good qubit or bad one.

Relaxation and decoherence caused by coupling to environment make most physical systems behave like classical systems, except microscopic systems, such as atoms. However, superconducting circuits maintain quantum properties with macroscopic or mesoscopic size. The size is not the only difference between atoms and superconducting circuits. Parameter-controlling in superconducting circuits is easier than in atoms, and coupling between two superconducting circuits can be turned on and turned off at will. Well-designed superconducting circuits may have better coherence time than atoms do, providing more time for quantum computing. Preparing initial states and measuring final states are also easier in superconducting circuits. Because of those advantages, although there are still many obstacles in the way to practical application, studying superconducting circuits is one of the main streams in quantum information processing. [10–14]

In this chapter, I will start from the basics of a Josephson junction, an important element of superconducting circuits, and introduce two fundamental types of superconducting qubits and some advanced types of qubits.

## 2.1 Josephson junctions

The fundamental structure of a Josephson junction consists of a sandwich of two superconductors separated by an insulating layer, typically fabricated from oxidation of the superconductors, and thin enough to allow tunneling of discrete charges through the barrier. That is why a Josephson junction is also called a superconducting tunnel junction or a Josephson tunnel junction.

For the purposes of creating a two-level system which is isolated from and not by external excitation resonant with other energy levels, the harmonic system is not suitable, in which all of energy gaps are the same. A nonlinear system is required. A Josephson junction [15, 16] is the electronic circuit element that has nonlinear and non-dissipative properties at arbitrarily low temperatures. Because of the properties of nonlinearity, when the driving frequency $\omega$ is detuned from the natural oscillation frequency $\omega_0$, the system is very sensitive between two possible oscillation states that differ in amplitude and phase. So, a Josephson junction is an important element not only of creating a qubit but also of quantum readout measurement.

### 2.1.1 The Josephson effect

As stated above, a junction consists two strongly superconducting electrodes connected by a weak link. The weak link can be an insulating layer as Josephson originally proposed, or a normal metal layer made weakly superconductive by the so-called proximity effect, or simply a short, narrow constriction in otherwise continuous superconducting material [16]. According to quantum mechanics, the electrons would tunnel through the weak link or barrier layer. There are two effects of pair tunneling, DC and AC Josephson effects [15].

DC Josephson effect: a dc current flows across the junction in the absence of any electric or magnetic field. The relationship between the phase difference $\delta$ and the current $I$ of superconducting pairs across the junction is

$$I_J = I_c \sin \delta \ . \tag{2.1}$$

The critical current $I_c$ is the maximum zero-voltage superconducting current that can pass through the junction above which the superconducting state will become normal state. It is proportional to the transfer interaction. Because no voltage apply, the phase difference $\delta$ is a constant. For finite voltage situations involving the ac Josephson effect, a more complete description is required.

AC Josephson effect: when a dc voltage is applied across the junction, an ac current flows across the junction. The phase difference $\delta$ is no longer a constant. The relationship between voltage and phase difference is

$$\dot{\delta} = -2eV/\hbar \tag{2.2}$$

or

$$\delta(t) = -\frac{2e}{\hbar} \int_0^t V\,dt + \delta(0) \ . \tag{2.3}$$

and the superconducting current is

$$I_J = I_c \sin\left(\delta(0) - 2eVt/\hbar\right) \ . \tag{2.4}$$

Furthermore, considering more general cases, we can apply a time-dependent voltage, and write down the function in some significant symbols,

$$I_J(t) = I_c \sin \frac{\Phi_J(t)}{\varphi_o} = I_c \sin \delta(t) \ , \tag{2.5}$$

where the generalized flux is defined by $\Phi_J = \int_{-\infty}^{t} V(t')dt$ and $\varphi_0 = \hbar/2e$ is the reduced flux quantum, or $\varphi_0 = \Phi_0/2\pi$, where $\Phi_0$, $h/2e$, is the magnetic flux quantum.

Actually, phase difference is not a gauge-invariant quantity; for a given physical situation, there is not only one unique value of phase difference. Hence it cannot in general determine the current $I_J$, which is a well-defined gauge-invariant physical quantity. The phase difference mentioned before is not the real phase difference between two superconductor [16], defined by

$$\delta \equiv \delta' - \frac{2\pi}{\Phi_0} \int \mathbf{A} \cdot d\mathbf{l} \,. \tag{2.6}$$

where $\delta'$ is the real phase difference and the integration over the vector potential $\mathbf{A}$ is from one electrode of the weak link to the other. Thus, the difficulty is cured. In addition to curing the conceptual problem, the introduction of the gauge-invariant phase difference is the key to working out the effects in a magnetic field, which cannot be treated without introducing the vector potential $\mathbf{A}$.

## 2.1.2 A Josephson junction with a nonlinear inductance

At first, let's take a short review of a conventional inductance.

$$L = \Phi/I \quad \text{or} \quad I = \phi/L \,,$$

where $L$ is the inductance, $\Phi$ is the magnetic flux, and $I$ is the current.

We thus expand Eq. (2.5)

$$I_J(t) = \frac{1}{L}\Phi_J(t) - \frac{1}{6L_J\varphi_0^2}\Phi_J^3(t) + O[\Phi_J^5(t)] \tag{2.7}$$

or simply

$$I_J(t) = I_c \sin \delta(t) = I_c \left( \delta(t) - \frac{\delta^3(t)}{3!} + ... \right) \,. \tag{2.8}$$
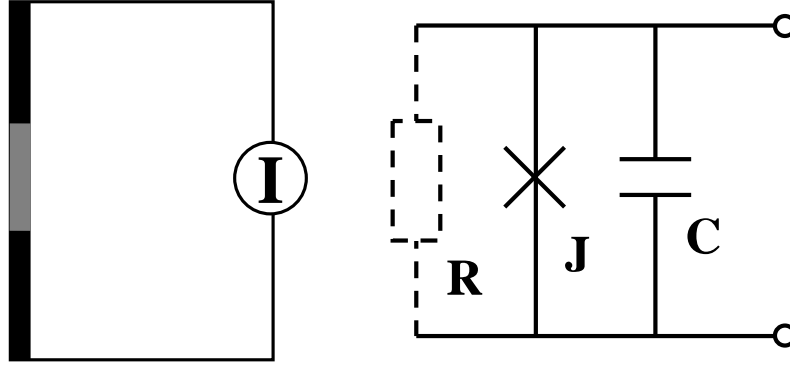
**Figure 2.1** The current-biased josephson junciton and its equivlent circuit.

By comparing the functions of a Josephson junction and a conventional inductance, it is very easy to find that besides the linear term in the relation of current and magnetic flux, there are additional nonlinear high-order terms in a Josephson junction. A Josephson junction, therefore, can be considered having a nonlinear inductance.

### 2.1.3   The current-biased Josephson junction

A Josephson junction schematically shown in Fig. 2.1 as a sandwich structure can be modeled as a parallel circuit which consists of a nonlinear inductance, a resistance, and a capacitance.

According to Kirchhoff's rule and some relationships, $I = C\dot{V} = C\ddot{\delta}, \delta = \frac{2e}{\hbar}\Phi$, and $I_j = I_c \sin \delta$, the equation of the circuit is

$$\frac{\hbar}{2e}C\ddot{\delta} + \frac{\hbar}{2eR}\dot{\delta} + I_c \sin \delta = I_e , \qquad (2.9)$$

where C is the capacitance, R is the resistance, and $V$ is the voltage across the capacitance. Then, it is useful to define some meaningful parameters, $E_C \equiv \frac{(2e)^2}{2C}$ and
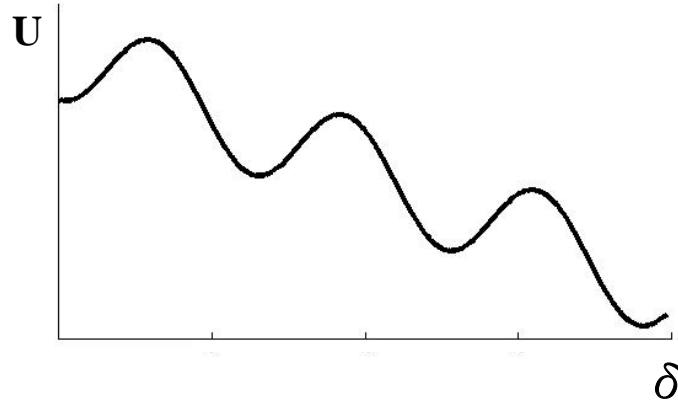
**Figure 2.2** The "tilted-washboard" effective potential versus phase difference of a current-biased Josephson junction.

$E_J \equiv \frac{\hbar}{2e} I_c$. The kinetic energy of the quasi-partical of phase $\delta$ is

$$K(\dot{\delta}) = \frac{\hbar^2 \dot{\delta}^2}{4E_C} , \tag{2.10}$$

the potential energy of it is

$$U(\delta) = E_J(1 - \cos \delta) - \frac{\hbar}{2e} I_e \delta , \tag{2.11}$$

and the Hamiltonian has the form

$$H = E_C n^2 - E_J \cos \delta - \frac{\hbar}{2e} I_e \delta . \tag{2.12}$$

The relationship of potential versus phase is shown in Fig. (2.2). It is obvious that nonlinear inductance, $\cos \delta$, makes potential oscillate and bias current makes it slope. When current bias is applied, the pendulum potential becomes tilted. By the way, a current-biased Josephson junction can be considered as a qubit, because the potential is cosine function, making energy gaps different.
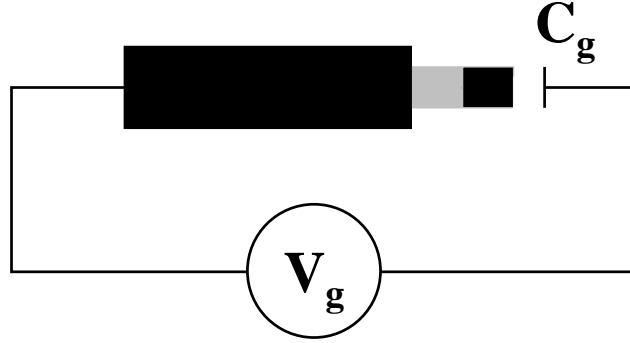
**Figure 2.3** The single Cooper pair box. One side of a small superconducting island is connected via a Josephson tunnel junction to a large superconducting reservoir, and another side is coupled capacitively to a voltage source.

## 2.2 The Cooper-pair box and the SQUID

### 2.2.1 The single cooper-pair box device

There is a small superconducting island in a superconducting Cooper-pair box (SCB) device as shown in Fig. 2.3. One side of the island is connected via a Josephson tunnel junction to a large superconducting reservoir, and the other side is coupled capacitively to a voltage source. Cooper pairs can only transfer to the island one by one in the device. The number of electrons on the island is controlled by the bias voltage.

The Hamiltonian of the cooper-pair box is

$$\hat{H} = E_C \left( \hat{n} - n_g \right)^2 - E_J \cos \hat{\delta} , \tag{2.13}$$

where $n_g = C_g V_g / 2e$ is the offset Cooper pair number caused by the gate voltage $V_g$ through gate capacitance $C_g$, and $n$ is the number of extra Cooper pairs between the two capacitances, the gate capacitance and the capacitance in the Josephson junction. Therefore, the first term, $E_C \left( \hat{n} - n_g \right)^2$, represents the electrostatic energy of
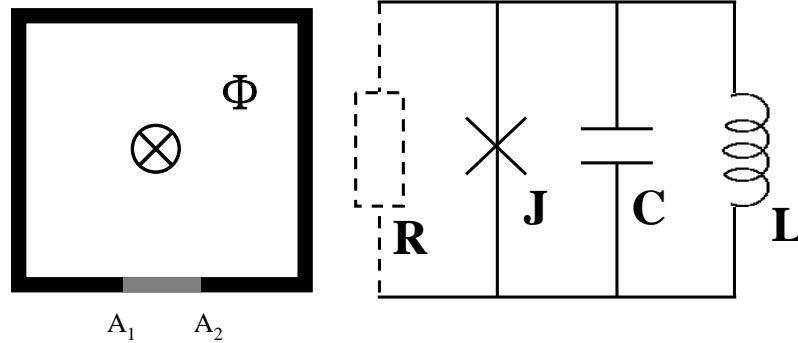
**Figure 2.4** The superconducting quantum interference device, SQUID, and its equivalent circuit.

the island, where $E_C = (2e)^2 / 2 (C + C_g)$. Due to the nonlinear inductance of the Josephson junction, the second term, $E_J \cos \hat{\delta}$, appears.

### 2.2.2   The SQUID device

A superconducting quantum interference device (SQUID) is a device involved with quantum interference.

A rf-SQUID, shown in Fig. 2.4, consists of a superconducting loop interrupted by a tunnel junction. a external magnetic flux is sent through the loop, inducing quantum interference.

According to the Meissner effect, we have

$$J(\mathbf{r}) = |\psi(r)|^2 \left[ \frac{q\hbar}{m^*} \nabla \theta(\mathbf{r}) - \frac{q^2}{m^* c} \mathbf{A}(\mathbf{r}) \right] , \qquad (2.14)$$

where $\mathbf{A}$ is the vector potential and $q \equiv -2e$ for a Cooper pair. Inside a superconductor, the current vanlishs,

$$\nabla \theta(\mathbf{r}) = -\frac{2e}{\hbar c} \mathbf{A}(\mathbf{r}) . \qquad (2.15)$$

Choosing a contour inside the superconducting loop, with Eq. (2.6) we can get

$$
\begin{aligned}
\Phi_t = \oint \mathbf{A} \cdot d\mathbf{l} &= \int_{A_1}^{A_2} \mathbf{A} \cdot d\mathbf{l} + \int_{A_2}^{A_1} \mathbf{A} \cdot d\mathbf{l} \\
&= -\frac{2e}{\hbar c} \int_{A_1}^{A_2} \nabla \theta(\mathbf{r}) \cdot d\mathbf{l} + \int_{A_2}^{A_1} \mathbf{A} \cdot d\mathbf{l} \\
&= \frac{2e}{\hbar c} \delta \ ,
\end{aligned}
\tag{2.16}
$$

where $\Phi_t$ is total magnetic flux and Eq. (2.6) has been used.

With magnetic flux $\Phi = \Phi_t - \Phi_e$ where $\Phi_e$ is external magnetic flux and the inductance energy $\frac{\Phi^2}{2L}$, the Hamiltonian of a rf-SQUID is given by

$$
\hat{H} = E_C \hat{n}^2 - E_J \cos \hat{\delta} + E_L \frac{(\hat{\delta} - \delta_e)^2}{2},
\tag{2.17}
$$

where $\delta_e = \frac{2e}{\hbar} \Phi_e$. The first term $E_C \hat{n}^2$ is electrostatic energy of the capacitance in the Josephson junction, and the second term is related to the Josephson energy. The last term corresponds to the inductance energy of the loop, and $E_L = \frac{\Phi_0^2}{4\pi^2 L}$. In the next part, another device, a dc-SQUID, and a very important concept related to it will be introduced.

A dc-SQUID is a device which consists of two tunnel junctions in a superconducting loop and is biased by an external current. It is similar to a current-biased Josephson junction with a two-junction loop, as shown in Fig. 2.5, instead of a single junction.

Two superconducting phases, $\delta_{1,2}$, is involved, and according to Eq. (2.5), the external current is

$$
I_{c1} \sin \delta 1 - I_{c2} \sin \delta 2 = I_e \ .
\tag{2.18}
$$
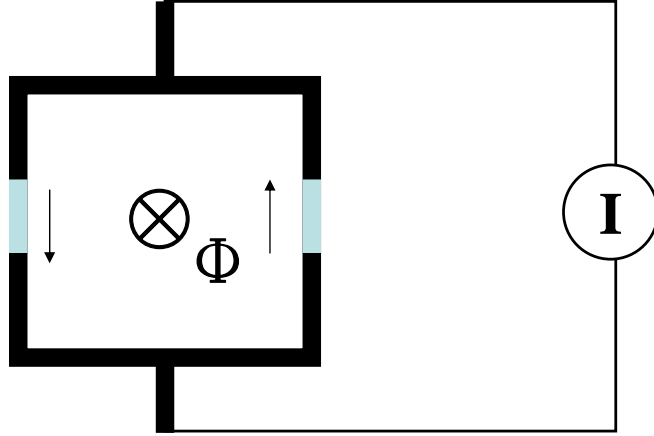
**Figure 2.5** The dc-SQUID. A superconducting loop with two Josephson junctions replaces the single junction in the current-biased Josephson junction circuit.

It is convenient to define some new variables,

$$\delta_{\pm} = \frac{\delta_1 \pm \delta_2}{2}, \tag{2.19}$$

and in a symmetric case, which the two Josephson junction are the same $I_{c1} = I_{c2}$, Eq. (2.18) reduces to the form

$$2I_c \cos\left(\delta_e/2\right) \sin\delta_- = I_e . \tag{2.20}$$

Comparing Eq. (2.20) with Eq. (2.5), we can find that $2I_c \cos\left(\delta_e/2\right)$ is the effective critical current. Most importantly, it can be tuned by the external magnetic flux and consequently the effective Josephson energy, $E_J = \frac{\hbar}{2e} 2I_c \cos\left(\delta_e/2\right)$ is tunable too. The Hamiltonian can be written by generalizing Eqs. (2.12),(2.17) for the phases $\delta_{\pm}$.

$$H = E_C \hat{n}_+^2 + E_C \hat{n}_-^2 - 2E_J \cos\hat{\delta}_+ \cos\hat{\delta}_- + E_L \frac{\left(2\hat{\delta}_+ - \delta_e\right)^2}{2} + \frac{\hbar}{2e} I_e \hat{\delta}_- , \tag{2.21}$$

where $\hat{n}_+$ and $\hat{n}_-$ are the conjugate momentum of $\hat{\delta}_+$ and $\hat{\delta}_-$. According to quantum mechanics-just like the familiar position and momentum operators $\hat{x}$ and $\hat{p}_x$-the

operators $\hat{\delta}$ and Cooper-pair number operator $\hat{n}$ on the capacitor are canonically conjugate, as expressed by the commutator braket, $[\hat{\delta}, \hat{n}] = i$.

## 2.3 Charge qubits and flux qubits

### 2.3.1 Charge qubits

A superconducting Josephson junction qubit in which the charging energy is much large than the Josephson coupling, $E_C \gg E_J$, is called a charge qubit. In this regime, a convenient basis is formed by the charge states, and the phase terms can be considered as perturbation. This is why this kind of qubits are called charge qubits. The necessary of one-qubit and two-qubit gates can be performed by controlling applied gate voltages and magnetic fields. Different designs will be presented that not only in complexity, but also in flexibility of manipulations.

In this subsection, the simplest charge qubit, cooper-pair box, Fig. 2.3, is presented in details. This example illustrates how charge qubits provide two energy states, which satisfy the requirements of qubits.

In charge regime, at first we expand all operators in the basis of the charge states $\{|n\rangle\}$. The Hamiltonian of a cooper-pair box, Eq. (2.13), is

$$\hat{H} = E_C \left( \hat{n} - n_g \right)^2 - E_J \cos \hat{\delta} \ .$$

Then by using the properties of orthonomal and complete set, $\langle n \mid \hat{n} \mid n' \rangle = \delta_{n,n'}$ and $I = \sum_n |n\rangle\langle n|$, the first term is rewritten as

$$\sum_n E_C \left( n - n_g \right)^2 |n\rangle\langle n| \tag{2.22}$$

and by using the commutator relation,

$$\left[\hat{\delta}, \hat{n}\right] = i \ ,$$

$$\Rightarrow \qquad \left[\hat{\delta}^m, \hat{n}\right] = im\hat{\delta}^{m-1} \ , \quad m > 0 \ ,$$

$$\Rightarrow \qquad \left[\hat{n}, e^{i\hat{\delta}}\right] = \left[\hat{n}, \sum_m \frac{\left(i\hat{\delta}\right)^m}{m!}\right] = e^{i\hat{\delta}} \ . \tag{2.23}$$

The commutator relation Eq. (2.23) is similar to the commutator relation of number operator $\hat{a}^+\hat{a}$ and the creation operator $\hat{a}^+$, $[\hat{a}^+\hat{a}, \hat{a}^+] = \hat{a}^+$. So, $e^{i\hat{\delta}}$ and $e^{-i\hat{\delta}}$ can be presented in charge basis,

$$e^{i\hat{\delta}} = \sum_n |n+1\rangle\langle n| \ , \ e^{-i\hat{\delta}} = \sum_n |n\rangle\langle n+1| \ , \tag{2.24}$$

and the second term of Eq. (2.13) is

$$\frac{1}{2}E_J \sum_n \left(|n\rangle\langle n+1| + |n+1\rangle\langle n|\right) \ . \tag{2.25}$$

By combining Eq. (2.22) and Eq. (2.25), in this basis the Hamiltonian reads

$$\hat{H} = \sum_n \left\{ E_C \left(n - n_g\right)^2 |n\rangle\langle n| - \frac{1}{2}E_J \left(|n\rangle\langle n+1| + |n+1\rangle\langle n|\right) \right\} \ . \tag{2.26}$$

The energy spectrum of Eq. (2.26) is shown in Fig. 2.6a.

Under suitable conditions, when charge number on a gate capacitor $n_g$ controlled by gate voltage $V_g$ equals half integers, the lowest two energy states are well-isolated from other states, shown in Fig. 2.6b. Because of that, near $n_g = 1/2$, the Hamiltonian can be reduced to

$$\hat{H} = -\frac{1}{2}\left(\epsilon\sigma_z + \Delta\sigma_x\right) \ , \tag{2.27}$$

where $\epsilon = E_C \left(1 - 2n_g\right)$, and $\Delta = E_J$. The qubit eigenenergies are then given by the equation

$$E_{1,2} = \mp\frac{1}{2}\sqrt{E_C^2 \left(1 - 2n_g\right)^2 + E_J^2} \ . \tag{2.28}$$

(a)  (b)
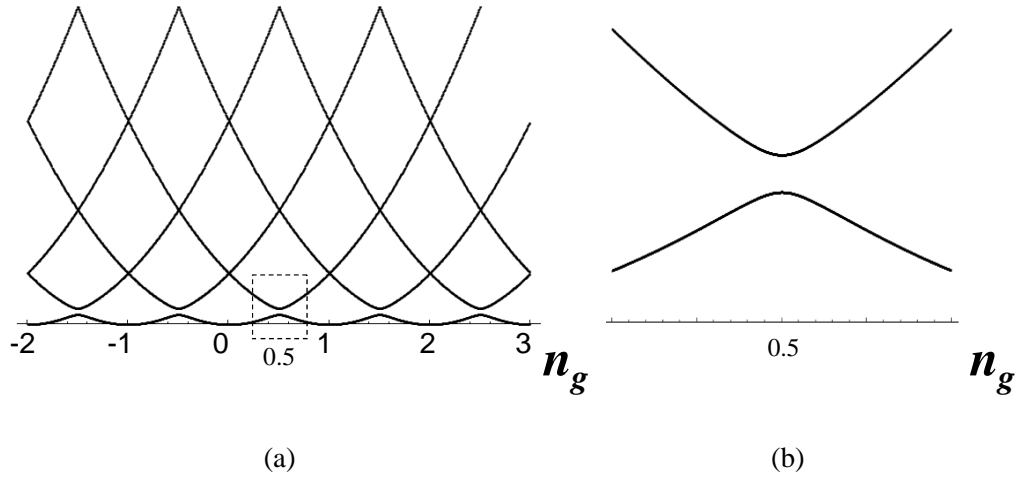
**Figure 2.6** (a) The energy spectrum of a charge qubit versus gate voltage. (b) The lowest two energy levels near $V_g = 0.5$, the part of (a) circumscribed by dashed lines.

So, under suitable conditions charge qubits provide physical realizations of qubits with two charge states differing by one cooper-pair charge on a small island. For quantum computation, it is required to have the ability to rotate a state on the Bloch sphere to any position at will, and consequently $\sigma_z$ and $\sigma_x$ rotation are necessary. In a cooper-pair box, pure $\sigma_x$ rotation is acquirable, as $n_g = 1/2$, but pure $\sigma_z$ rotation is not, since $E_J$ is fixed. In previous section, an important concept is mentioned. A two-junction loop can substitute for the single Josephson junction, creating a SQUID-controlled qubit, Fig. 2.7. Thus, the effective Josephson energy $E_J$ is tunable and pure $\sigma_z$ rotations can be performed.

## 2.3.2  Advanced charge qubits

Operated in $E_J/E_C \ll 1$ regime, basic charge qubits have good anharmonicity to form two-level systems but their energy bands shown in Fig. 2.6 have slopes, making them very sensitive to low-frequency charge noise. The magnitudes of charge dispersion and
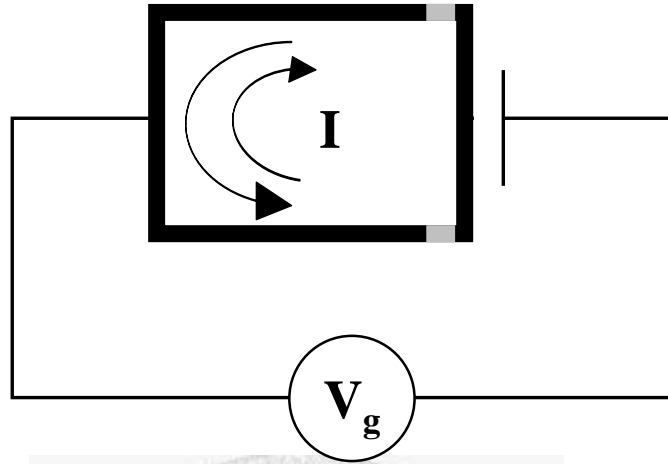
**Figure 2.7** The single Cooper pair transistor. A superconducting loop with two Josephson junctions replaces the single junction in a SCB for a tunable $E_J$.

anharmonicity are both determined by the ratio $E_J/E_C$. The low value of the ratio of $E_J/E_C$ brings not only good manipulations of qubits but also serious decoherence. Many researchers keep trying to find solutions for this problem. A famous example is the transmon [17], Fig. 2.8. The fundamental idea of the transmon is to shunt the Josephson junction of a small Cooper-pair box with a large external capacitor to increase the charging energy $E_C$ and to increase the gate capacitor to the same size. This make the charge dispersion reduces exponentially in $E_J/E_C$, while the anharmonicity only decreases algebraically with a slow power law in $E_J/E_C$.

### 2.3.3 Flux qubits

In the previous section, we describe the quantum dynamics of low-capacitance Josephson devices where the charging energy dominates over the Josephson energy, $E_C \gg E_J$, and the relevant quantum degree of freedom is the charge on superconducting
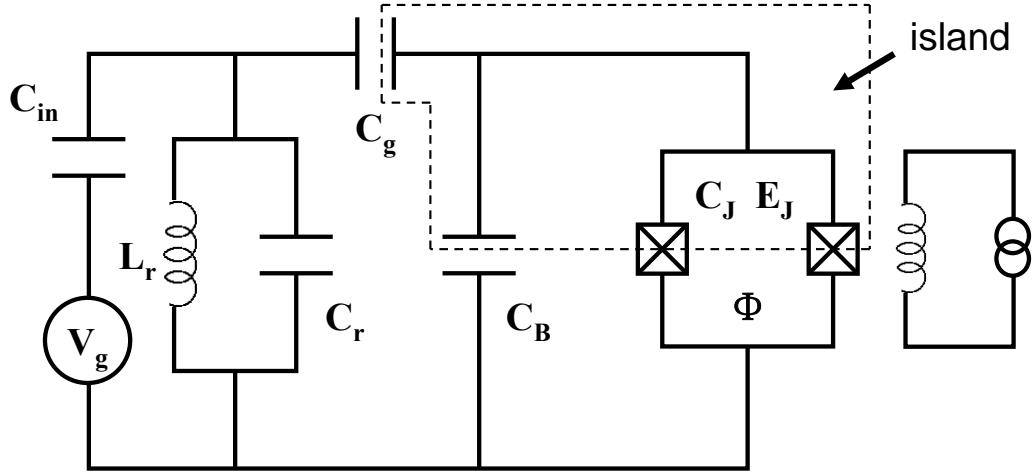
**Figure 2.8** The equivalent circuit of a transmon.

island. We now talk about another quantum regime, the phase regime, $E_J \gg E_C$, in which the flux states are the better basis. This kind of qubits are called flux qubits.

A rf-SQUID is the simplest example of a flux qubit. The Hamiltonian, Eq. (2.17), is

$$\hat{H} = E_C \hat{n}^2 - E_J \cos \hat{\delta} + E_L \frac{(\hat{\delta} - \hat{\delta}_e)^2}{2} \ ,$$

and in the phase regime, the potential energy is given by

$$U(\delta) = -E_J \cos \delta + E_L \frac{(\delta - \delta_e)^2}{2} \ . \tag{2.29}$$

The potential energy is cosine function added a second power function. $\delta_e$ in a flux qubit play as the same role as $n_g$ do in a charge qubit. The lowest area can be approximated to a double-well. When $\delta_e$ equals $\pi$ or odd $\pi$, a symmetric double-well potential energy appears. It is similar to that of $n_g$ equal $1/2$ in a charge qubit. Because of the tunneling through center barrier, the lowest two energy level split with a gap $\Delta$, which depends on the height of the barrier. When $\delta_e$ doesn't equal $\pi$

or odd $\pi$, the potential energy becomes unsymmetric, the probability of the lowest energy pair is not half in each well. This situation is like when $n_g$ is near $1/2$, in a charge qubit, the probability is not the same in $|0\rangle$ and $|1\rangle$. The Hamiltonian of a flux qubit can be truncated to the lowest two energy states in a simple form of

$$\hat{H} = -\frac{1}{2}\left(\epsilon\sigma_z + \Delta\sigma_x\right) , \tag{2.30}$$

where $\Delta$ depends on $E_J$ and $\epsilon$ is given by

$$\epsilon = 4\pi\sqrt{6\left(\frac{E_J}{E_L} - 1\right)E_J}\left(\frac{\Phi_e}{\Phi_0} - \frac{1}{2}\right) . \tag{2.31}$$

In this form, the pure operator X-rotation can be performed by setting $\Phi/\Phi_e = 1/2$, but the pure Z-rotation can not. In order to solve this problem, we can replace the single junction with a two-junciton loop that introduces an additional external flux $\tilde{\Phi}_e$ as another control variable. Therefore, the effective Josephson energy becomes tunable.

### 2.3.4 Advanced flux qubits

The main idea in a SQUID is to create a double-well potential, requiring large enough inductance. This implies that the qubit contains a large qubit loop, making itself influenced by magnetic fluctuations of environment seriously. One way to overcoming this difficulty is using a three-junction device pointed out by Mooij *et al.* [18]. In a three-junction-loop qubit, as shown in Fig. 2.9, $E_L$ is not the only element to creating a double-well potential. The loop, therefore, can be much small than a rf-SQUID and the qubit is relatively free from charge and magnetic environment fluctuations.
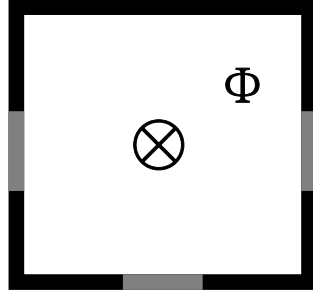
**Figure 2.9** The three-junction SQUID.

# 2.4 The quantronium

With device parameters locating between charge qubits and flux qubits, the quantronium [19, 20] is a very special kind of qubits. Neither $\hat{n}$ nor $\hat{\delta}$ is a good quantum number since the quantronium is operated in $E_J \cong E_C$ regime. The circuit of a quantronium is shown in Fig. 2.10. the island connected to two Josephson junctions and a voltage is applied to it through a capacitance. The two small Josephson junctions and a large Josephson junction with a higher critical current $E_{J0} \approx 20E_J$ form a closed loop, and an external magnetic flux is applied to it. The two small junctions define the superconducting island of the box, and the phase $\hat{\gamma}$ of the large junciton, so-called read-out junciton, coupled to the qubit. A readout pulse current $I_b(t)$, with a peak value approaching the large junciton's critical current, is applied to the parallel combination of the large junction and the small junctions. If the state of the qubit is $|1\rangle$, the supercurrent adds the readout pulse will make the large junction switch to a finite voltage state. If the state of the qubit is $|0\rangle$, the large junciton will stay in the superconducting zero voltage state.

When the qubit operates in the charge-flux regime, $E_J \cong E_C$, no matter charge or flux noise decoherence can be reduced to higher order, because the slope of energy
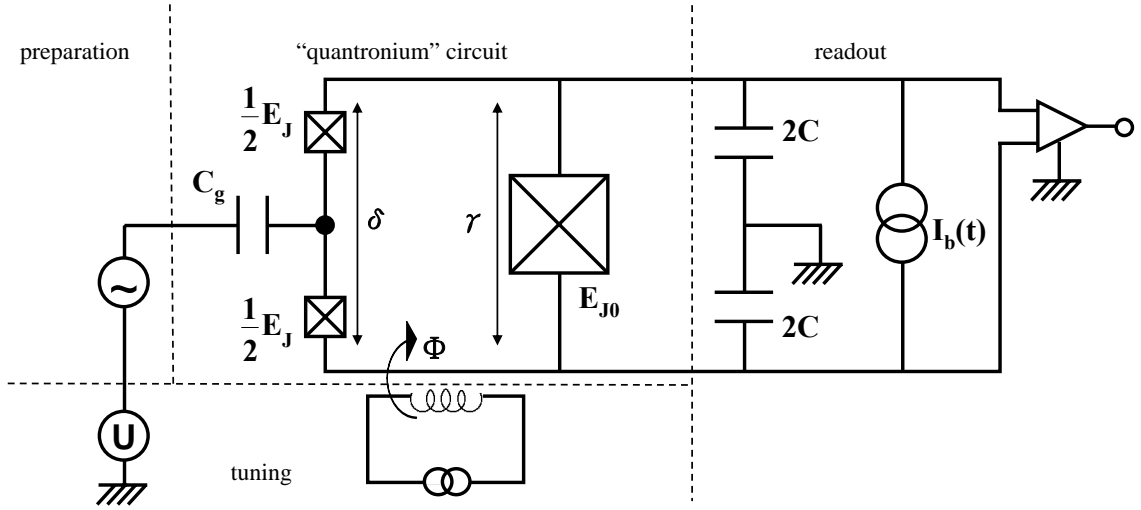
**Figure 2.10** The circuit diagram of the quantronium with preparation, tuning, readout blocks.

levels in the charge degree of freedom and in the flux degree of freedom are both flatter than simple charge qubits and flux qubits. Moreover, if the qubit is maintained at the double degeneracy point, $n_g = 1/2$ and $\Phi = 0$, the influence of both flux and charge noise sources vanishes to first order.

## 2.5 The Josephson bifurcation amplifier

In this section, we will introduce briefly the Josephson bifurcation amplifier designed to measure the states of charge qubits. In order to measure the state of a charge qubit, the number of Cooper-pairs, we need a very sensitive device and the accuracy of it must much bigger than $2e$. Before the Josephson bifurcation amplifier, there are many measurement devices such as the single-electron transistor (SET) or the readout junction of quantronium, but in those devices, the dissipation problem is usually serious, because they are involved with switching to finite voltage states. This flaw was conquered by the introduction of the Josephson bifurcation amplifier (JBA). I.

Siddiqi *et al.* [7] constructed a new type of amplifiers based on the transition of a rf-driven Josephson junction between two distinct oscillation states near a dynamical bifurcation point. The main advantages of JBA are speed, high secsitivity, low backaction, and the most special character is the absence of on-chip dissipation. The measurement of quantronium with JBA [21] was published by I. Siddiqi *et al.* some years later and quantum nondemolition readout using a JBA [22, 23] was also published by I. Siddiqi *et al.* soon.

The central element of a JBA is a Josephson junction whose critical current $I_0$ can be modulated by an input signal, i.e. states of a qubit. Another sinusoidal signal drives this Joseson junction. An output port is connected to this circuit to measure the reflected component of the drive signal. Simply, a JBA is a driven Josephson junction with a tunable critical current. The anharmonic potential of the Josephson junction and the sinusoidal driving make up a famous mathematical model, the Duffing oscillator, which have two distinct possible oscillation states that differ in amplitude and phase.

### 2.5.1 The quantronium with a JBA readout

Figure 2.11 is a quantronium circuit with preparation and readout ports [22]. The middle part is a quantronium qubit. The two parallel Josephson junctions have capacitances $C_J/2$ and Josephson energies $E_J(1 \pm d)/2$, where $d$ is the asymmetry factor quantifying the difference between the two junctions ($0 \leq d \leq 1$), and $E_J = \varphi_0 I_0$, where $I_0$ is the sum of critical currents of the junctions. The island is biased by a voltage source $V_{g0}$ in series with a gate capacitance $C_g$. The Hamiltonian of the
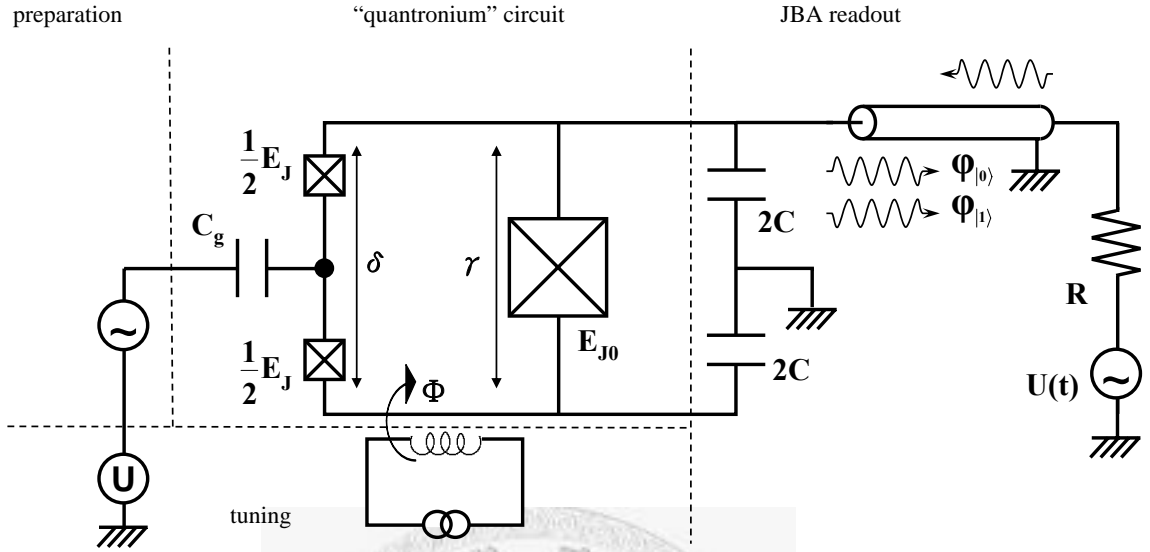
**Figure 2.11** Quantronium circuit with JBA readout port. A JBA readout port replaces the voltage-switching measurement in the original design of the quantronium.

quantronium is

$$H = E_{CP} \left( \hat{n} - n_g \right)^2 - E_J \left( \cos \frac{\delta}{2} \cos \hat{\theta} - d \sin \frac{\delta}{2} \sin \hat{\theta} \right) \ , \qquad (2.32)$$

where $E_{CP} = (2e)^2/2(C_g + C_J)$, $\hat{\theta}$ is the superconducting operator ("conjugate" to $\hat{n}$—i.e., $[\hat{\theta}, \hat{n}] = i$), and $\delta$ is the superconducting phase across the series combination of the two small junctions. $n_g$ and $\delta$ can be tuned by biased voltage and external flux, respectively, and the energy spectrum is sufficiently anharmonic, i.e. the gaps between any two energy levels are strongly unequal. This suggests that the first two energy states can form a qubit.

For the purpose of measurement, a JBA readout device is coupled to the quantro-

nium. The total Hamiltonian with the external flux $\Phi = 0$ is

$$H_{tot} = E_{CP}\left(\hat{n} - n_g\right)^2 - E_J\left[\cos\hat{\theta} \otimes \cos\frac{\hat{\delta}}{2} - d\sin\hat{\theta} \otimes \sin\frac{\hat{\delta}}{2}\right]$$

$$+ \frac{\hat{Q}^2}{2C} - E_{J0}\cos\hat{\delta} - \frac{U(t)}{R}\varphi_0\hat{\delta}\,, \tag{2.33}$$

where $E_{J0}$ is the Josephson energy of the readout junction and $U(t)$ is a time-dependent driving potential. To study a measurement problem, it is very convenient to rewrite the Hamiltonian in the following form,

$$H_{tot} = H_S + H_I + H_P\,, \tag{2.34}$$

where $H_S$ is the Hamiltonian of system, i.e. the quantronium, $H_P$ is the Hamiltonian of the probe, i.e. the JBA, and $H_I$ is their interaction Hamiltonian. So Eq. (2.33) is rewritten as

$$\begin{aligned} H_{tot} &= H_S + H_I + H_P \\ &= E_{CP}\left(\hat{n} - n_g\right)^2 - E_J\cos\hat{\theta} \\ &\quad - E_J\left\{\cos\hat{\theta} \otimes \left[\cos\frac{\hat{\delta}}{2} - 1\right] - d\sin\hat{\theta} \otimes \sin\frac{\hat{\delta}}{2}\right\} \\ &\quad + \frac{\hat{Q}^2}{2C} - E_{J0}\cos\hat{\delta} - \frac{U(t)}{R}\varphi_0\hat{\delta}\,. \end{aligned} \tag{2.35}$$

To approximate a two-level system, the Hamiltonian at the optimum $n_g = 1/2$ is truncated to

$$\begin{aligned} H_S &= -\frac{\hbar\omega_{01}}{2}\sigma_z\,, \\ H_I &= -\left\{\alpha\sigma_z \otimes \left[\cos\frac{\hat{\delta}}{2} - 1\right] - \beta\sigma_y \otimes \sin\frac{\hat{\delta}}{2}\right\}\,, \\ H_P &= \frac{\hat{Q}^2}{2C} - E_{J0}\cos\hat{\delta} - \frac{U(t)}{R}\varphi_0\hat{\delta}\,, \end{aligned} \tag{2.36}$$

where $\alpha = E_J(\langle 0|\cos\hat{\theta}|0\rangle - \langle 1|\cos\hat{\theta}|1\rangle)/2$ and $\beta = idE_J(\langle 0|\sin\hat{\theta}|1\rangle - \langle 1|\sin\hat{\theta}|0\rangle)/2$. With $d = 0$, the requirement $[H_S, H_I] = 0$ of a quantum non-demolition (QND) is

fulfilled. The qubit in this case is coupled to the JBA through only a $\sigma_z$ operator.

If $\cos\hat{\delta}$ in $H_P$ is expanded to the order of $\hat{\delta}^4$, we then have a system of a nonlinear driven quantum Duffing oscillator. In the following chapters, we will discuss the properties of a driven quantum Duffing oscillator in order to understand the behavior of the JBA. The time-dependent driving, $U(t)$ in Eq. (2.36), is a generally a periodic in time function. So, we will describe in the next chapter a formalism, known as the Floquet formalism, to deal with the periodic in time problem.

# Chapter 3

# The Floquet formalism

Originally, the Flouqet theory is a mathematical theory dealing with differential equations. In 1965, Jon H. Shirley introduced this method to solve the Schrödinger equation with periodic in time [24]. By using the method of separation variables, a time-independent Schrödinger equation becomes an eigenvalue-eigenfunction equation, $\hat{H} |\psi_\alpha\rangle = E_\alpha |\psi_\alpha\rangle$. After getting the eigenenergies and eigenvectors, the time evolution of states is easily solved, $|\Psi_\alpha(t)\rangle = \sum C_\alpha e^{-iE_\alpha t} |\psi_\alpha\rangle$. However, there is no well-defined eigenenergy and eigenvector with a time-dependent Hamiltionian, which means there is no stationary state, and a time-ordered integral form, $\hat{T}[e^{\int H dt}]$, is always involved in the time evolution of states. According to the Flouqet theorem, if a time-periodic system is expanded in a time-space Hilber space, the time-periodic Schrödinger equation becomes an eigenvalue-eigenfunction equation, too. Therefore, the knowledge of the time-independent Schrödinger equation can be used in time-dependent one. Besides, there are many advantages for different cases using the Floquet theory [25, 26].

In this chapter, we try to introduce the basic concepts of the Flouqet theory and

show two examples, a two-level system and a nonlinear oscillator, with periodic in time driving. First, a general form of the solution in the Floquet theory is introduced and determined. Besides, any operator with either time-dependent or time-independent terms, is presented in the Floquet picture as a time-indenpendent operator. As a result, the time-dependent Hamiltonian can be transformed to a time-independent matrix in the Floquet picture. Therefore, how to solve the time-dependent Schrödinger equation becomes a pure eigenvalue-eigenvector question. Finally, the time evolution of states can be obtained.

## 3.1 The Flouqet theory

### 3.1.1 General form of the solution

Suppose there is a Schrödinger equation with a periodic Hamiltonian,

$$i\frac{d}{dt}|\Psi(t)\rangle = \hat{H}(t)|\Psi(t)\rangle , \tag{3.1}$$

where $H$ is a Hermitian matrix of period functions of t with a period $\tau$, $\hat{H}(t-\tau) = \hat{H}(t)$ . The general form of the solution of a differential equation with periodic coefficients is given by Floquet's theorem. So, the Floquet theorem asserts that the solutions of the Schrödinger equation (3.1) in a time-periodic potential with a period $\tau$, can be described as a linear combination of the qusienergy states (QES) $|\psi_\alpha(t)\rangle$, That is $|\Psi(t)\rangle$ which satisfies Eq. (3.1) can be written as

$$|\Psi(t)\rangle = \sum_\alpha C_\alpha |\psi_\alpha(t)\rangle , \quad |\psi_\alpha(t)\rangle = e^{-i\epsilon_\alpha t}|\phi_\alpha(t)\rangle , \tag{3.2}$$

where $|\phi_\alpha(t)\rangle$ is a periodic state, $|\phi_\alpha(t+\tau)\rangle = |\phi_\alpha(t)\rangle$, and $\epsilon$ is a real parameter called the quasienergy. The Floquet theorem for time-periodic problems is similar to the Bloch theorem for a space-periodic problems in Solid-state physics. The role of

the quasienergy $\epsilon$ in the Floquet theorem is therefore similar to that of the quasimo-mentum in the Bloch theorem.

Now, the next goal is to find a equation for the QES $|\psi_\alpha(t)\rangle$. Defining

$$\hat{F} \equiv \hat{H} - i\frac{d}{dt} \tag{3.3}$$

and substituting Eq. (3.2) into Eq. (3.1) reveals that

$$\hat{F}(t)|\psi_\alpha(t)\rangle = 0$$

$$\Rightarrow \quad \hat{F}(t)e^{-i\epsilon_\alpha t}|\phi_\alpha(t)\rangle = 0$$

$$\Rightarrow \quad e^{-i\epsilon_\alpha t}\hat{H}(t)|\phi_\alpha(t)\rangle - e^{-i\epsilon_\alpha t}i\frac{d}{dt}|\phi_\alpha(t)\rangle - |\phi_\alpha(t)\rangle i\frac{de^{-i\epsilon_\alpha t}}{dt} = 0$$

$$\Rightarrow \quad \hat{F}(t)|\phi_\alpha(t)\rangle = \epsilon_\alpha|\phi_\alpha(t)\rangle . \tag{3.4}$$

Equation (3.4) seems like an eigenvalue-eigenfunction equation. If a suitable basis can be found, it is just required to solve an eigenvalue-eigenfunction equation instead of a time-dependent Schrödinger equation. In this case, using the eigenvalue $\epsilon_\alpha$, the eigenvector $|\phi_\alpha(t)\rangle$ and Eq. (3.2), we can get the evolution of all states.

### 3.1.2 Some properties of quasienergy and QES

If $\epsilon_\alpha$ is one of the quasienergies and $|\phi_\alpha(t)\rangle$ is the corresponding quasieigenvector, considering the follow transform,

$$\epsilon'_{\alpha,m} \equiv \epsilon_\alpha + m\omega , \tag{3.5}$$

$$|\phi'_\alpha(t)\rangle \equiv e^{im\omega}|\phi_\alpha(t)\rangle , \tag{3.6}$$

where $\omega = 2\pi/\tau$. This can be checked by substituting them into Eq. (3.2). We then can find that the QES $|\psi_\alpha(t)\rangle$ is unchanged upon this transformation, and so is $|\Psi(t)\rangle$. This means if $\epsilon_\alpha$ is one of the quasienergies, so is $\epsilon_\alpha + m\omega$, and the Floquet

states are physically equivalent if their quasienergies differ by m$\omega$.

Because of the time-periodic properties, the Floquet states $|\phi_\alpha(t)\rangle$ can be expanded in Fourier series,

$$|\phi_\alpha(t)\rangle = \sum_{n=-\infty}^{\infty} |\phi_{\alpha,n}\rangle e^{-in\omega t} , \qquad (3.7)$$

with the Fourier components of the Floquet states

$$|\phi_{\alpha,n}\rangle = \frac{1}{\tau}\int_0^\tau dt e^{in\omega t}|\phi_\alpha(t)\rangle , \qquad (3.8)$$

and the QES

$$|\psi_\alpha(t)\rangle = e^{-i\epsilon_\alpha t}\sum_{n=-\infty}^{\infty}|\phi_{\alpha,n}\rangle e^{-in\omega t} . \qquad (3.9)$$

Finally, the total state $|\Psi(t)\rangle$, Eq. (3.2),

$$|\Psi(t)\rangle = \sum_{n,\alpha} C_\alpha e^{-i(\epsilon_\alpha+n\omega)t}|\phi_{\alpha,n}\rangle . \qquad (3.10)$$

Thus a state can be considered as a superposition of stationary states with energies equal to $(\epsilon_\alpha + n\omega)$. This is why we call $\epsilon_\alpha$ quasienergy.

The time-periodic Hamiltonian $\hat{H}(t)$ can also be expanded in Fourier series,

$$\hat{H}(t) = \sum_{n=-\infty}^{\infty}\hat{H}_n e^{-in\omega t} . \qquad (3.11)$$

and thus

$$\hat{F}(t) = \sum_{n=-\infty}^{\infty}\hat{H}_n e^{-in\omega t} - i\frac{d}{dt} . \qquad (3.12)$$

For the Hermitian oprator $\hat{F}$, one can introduce the composite Hilbert space which contains time-periodic wave fuction. The eigenvectors of $\hat{F}$ satisfy the orthonormality condition

$$\langle\phi_\alpha(t)|\phi_\beta(t)\rangle = \delta_{\alpha,\beta} , \qquad (3.13)$$

and form a complete set

$$\sum_\alpha |\phi_\alpha(t)\rangle\langle\phi_\alpha(t)| = I . \tag{3.14}$$

After using Eq. (3.12) and Eq. (3.7), another form of Eq.(3.4) is given,

$$\sum_{n',n} \left( \hat{H}_{n'} e^{-in'\omega t} - i\frac{d}{dt} \right) e^{-in\omega t} |\phi_{\alpha,n}\rangle = \epsilon_\alpha \sum_{n=-\infty}^{\infty} e^{-in\omega t} |\phi_{\alpha,n}\rangle ,$$

$$\Rightarrow \quad \sum_{n',n} \left( \hat{H}_{n'} e^{-i(n'+n)\omega t} - n\omega e^{-in\omega t} \right) |\phi_{\alpha,n}\rangle = \epsilon_\alpha \sum_{n=-\infty}^{\infty} e^{-in\omega t} |\phi_{\alpha,n}\rangle . \tag{3.15}$$

For the $m$th component,

$$\sum_{n',n} \left( \delta_{m,n'+n} \hat{H}_{n'} - n\omega\delta_{m,n} \right) |\phi_{\alpha,n}\rangle = \epsilon_\alpha |\phi_{\alpha,m}\rangle$$

$$\Rightarrow \quad \sum_n \left( \hat{H}_{m-n} - n\omega\delta_{m,n} \right) |\phi_{\alpha,n}\rangle = \epsilon_\alpha |\phi_{\alpha,m}\rangle . \tag{3.16}$$

Now, we can define $\hat{H}_{n'-n} \equiv \hat{H}_{n',n}$ and get

$$\sum_n \left( \hat{H}_{m,n} - n\omega\delta_{m,n} \right) |\phi_{\alpha,n}\rangle = \epsilon_\alpha |\phi_{\alpha,m}\rangle . \tag{3.17}$$

## 3.2 The extended Hilbert space

The above equation is formally equivalent to a time-independent Schrödinger equation and $\hat{F}$ is the Hermitian operator which determines the quasienergies and the Floquet states. The corresponding Hilbert space is the direct product $T \otimes R$ of the original Hilbert space $R$ and the Hilbert space of the time-periodic functions $T$. The inner product in $T$ is defined by

$$\langle n|m\rangle = \frac{1}{\tau} \int_0^\tau dt n^*(t) m(t) . \tag{3.18}$$

The most simple basis $\{|n\rangle\}$ of orthonormalized vectors for this space is the set of vectors defined by $\langle t|n\rangle = \exp[-in\omega t]$, and the spatial orthonormalized basis $\{|\beta\rangle\}$ is

chosen arbitrarily for convenience,

$$\langle \alpha m \mid \beta n \rangle = \langle \alpha \mid \beta \rangle \frac{1}{\tau} \int_0^\tau e^{im\omega t} e^{-in\omega t} dt = \delta_{\alpha\beta} \delta_{nm} \ , \tag{3.19}$$

and a time-periodic function is given by

$$|\Phi(t)\rangle = \sum_{\alpha m} f_{\alpha m} e^{-im\omega t} |\alpha\rangle = \sum_{\alpha m} f_{\alpha m} |\alpha m\rangle \ , \tag{3.20}$$

where

$$f_{\alpha m} = \int_0^\tau e^{im\omega t} f_\alpha dt \ . \tag{3.21}$$

### 3.2.1 Operators in the extended Hilbert space

In matrix form, any time-indepandent operator $A$ in the extended Hilbert space $T \otimes R$ is written as

$$I \otimes A = \begin{bmatrix} & & & \vdots & & & \\ A & 0 & 0 & 0 & 0 & & n = 2 \\ 0 & A & 0 & 0 & 0 & & n = 1 \\ \cdots & 0 & 0 & A & 0 & 0 & \cdots & n = 0 \\ 0 & 0 & 0 & A & 0 & & n = -1 \\ 0 & 0 & 0 & 0 & A & & n = -2 \\ & & & \vdots & & & \end{bmatrix} \ . \tag{3.22}$$

For a time-periodic operator with $\exp[-i\omega t]$ term, $B(t) = Ae^{-i\omega t}$, the matrix element of time doman is given by

$$\langle m|e^{-i\omega t}|n\rangle = \frac{1}{\tau} \int_0^\tau e^{im\omega t} e^{-i\omega t} e^{-in\omega t} dt = \delta_{m,n+1} \ . \tag{3.23}$$

For a time-periodic operator $C(t)$, $C(t) = Ae^{i\omega t}$, the matrix element of time doman is given by

$$\langle m|e^{i\omega t}|n\rangle = \frac{1}{\tau} \int_0^\tau e^{im\omega t} e^{i\omega t} e^{-in\omega t} dt = \delta_{m,n-1} \ . \tag{3.24}$$

$B(t)$ and $C(t)$ are written respectively as

$$
B(t) = \left[ \begin{array}{ccccc} & \vdots & & & \\ 0 & 1 & 0 & 0 & 0 \\ 0 & 0 & 1 & 0 & 0 \\ \cdots & 0 & 0 & 0 & 1 & 0 & \cdots \\ 0 & 0 & 0 & 0 & 1 \\ 0 & 0 & 0 & 0 & 0 \\ & \vdots & & & \end{array} \right] \otimes A \quad \text{and} \quad C(t) = \left[ \begin{array}{ccccc} & \vdots & & & \\ 0 & 0 & 0 & 0 & 0 \\ 1 & 0 & 0 & 0 & 0 \\ \cdots & 0 & 1 & 0 & 0 & 0 & \cdots \\ 0 & 0 & 1 & 0 & 0 \\ 0 & 0 & 0 & 1 & 0 \\ & \vdots & & & \end{array} \right] \otimes A \, .
$$

$$(3.25)$$

A simple concept here is that a $e^{i\omega t}$ term would "shift up" the spatial part a "block", a $e^{-i\omega t}$ term would "shift down" the spatial part a "block". Furthermore a $e^{2i\omega t}$ term 'shifts up' two block and so on.

Besides those operators, there is still another term, $id/dt$ in operator $\hat{F}$. Through the similar method, the matrix element of $id/dt$ is given by

$$
\left\langle m \left| i\frac{d}{dt} \right| n \right\rangle = \frac{1}{\tau} \int_0^\tau e^{im\omega t} i\frac{d}{dt} e^{-in\omega t} dt = n\omega \delta_{m,n} \, ,
$$

$$(3.26)$$

and in matrix form $id/dt$ is written as

$$
i\frac{d}{dt} = \left[ \begin{array}{ccccc} & \vdots & & & \\ 2\omega & 0 & 0 & 0 & 0 \\ 0 & \omega & 0 & 0 & 0 \\ \cdots & 0 & 0 & 0\omega & 0 & 0 & \cdots \\ 0 & 0 & 0 & -\omega & 0 \\ 0 & 0 & 0 & 0 & -2\omega \\ & \vdots & & & \end{array} \right]
$$

$$(3.27)$$

### 3.2.2 The Floquet Hamiltonian

Matrix elements of Hamiltonian, $\hat{H}(t) = \sum \hat{H}_{n'} e^{-in'\omega t}$, are

$$\left\langle m \middle| \hat{H}_{n'} e^{-in'\omega t} \middle| n \right\rangle = \sum_{n'} \hat{H}_{n'} \delta_{m,n+n'} = \hat{H}_{m-n} \tag{3.28}$$

$$
\hat{H}(t) = \begin{bmatrix}
& & & \vdots & & & \\
& H_0 & H_1 & H_2 & H_3 & H_4 & \\
& H_{-1} & H_0 & H_1 & H_2 & H_3 & \\
\cdots & H_{-2} & H_{-1} & H_0 & H_1 & H_2 & \cdots \\
& H_{-3} & H_{-2} & H_{-1} & H_0 & H_1 & \\
& H_{-4} & H_{-3} & H_{-2} & H_{-1} & H_0 & \\
& & & \vdots & & &
\end{bmatrix}, \tag{3.29}
$$

and by defining $\hat{H}_{n-m} \equiv \hat{H}_{m,n}$

$$
\hat{H}(t) = \begin{bmatrix}
& & & \vdots & & & \\
& H_{2,2} & H_{2,1} & H_{2,0} & H_{2,-1} & H_{2,-2} & \\
& H_{1,2} & H_{1,1} & H_{1,0} & H_{1,-1} & H_{1,-2} & \\
\cdots & H_{0,2} & H_{0,1} & H_{0,0} & H_{0,-1} & H_{0,-2} & \cdots \\
& H_{-1,2} & H_{-1,1} & H_{-1,0} & H_{-1,-1} & H_{-1,-2} & \\
& H_{-2,2} & H_{-2,1} & H_{-2,0} & H_{-2,-1} & H_{-2,-2} & \\
& & & \vdots & & &
\end{bmatrix}. \tag{3.30}
$$

Thus, the operator $\hat{F}$ can be expanded to an infinite time-independant matrix, called the Floquet Hamiltonian $\hat{H}_F$,

$$\hat{H}_F = \hat{H}(t) - i\frac{d}{dt}$$

$$= \left[ \begin{array}{ccccc} & & \vdots & & \\ H_{2,2} - 2\omega & H_{2,1} & H_{2,0} & H_{2,-1} & H_{2,-2} \\ H_{1,2} & H_{1,1} - \omega & H_{1,0} & H_{1,-1} & H_{1,-2} \\ \cdots \quad H_{0,2} & H_{0,1} & H_{0,0} + 0\omega & H_{0,-1} & H_{0,-2} \quad \cdots \\ H_{-1,2} & H_{-1,1} & H_{-1,0} & H_{-1,-1} + \omega & H_{-1,-2} \\ H_{-2,2} & H_{-2,1} & H_{-2,0} & H_{-2,-1} & H_{-2,-2} + 2\omega \\ & & \vdots & & \end{array} \right]$$

$$(3.31)$$

Equation (3.31) is the matrix form of Eq. (3.17). A time-dependent Hamiltonian (3.12) transforms to an infinite dimensional time-independent matrix, and its eigenvalues and eigenvectors are the quasienergies $\epsilon_\alpha$ and the quasivectors $|\phi_\alpha\rangle$, respectively.

## 3.3 Driven two-level systems and oscillators in the Floquet picture

### 3.3.1 Driven two-level systems

Considering a quantum system with two discrete states and letting an oscillating in time interaction connect these states with a matrix element $2B\cos\omega t$, where $B$ is a real number, we have the Hamiltonian,

$$\hat{H}(t) = \frac{1}{2}A\sigma_z + 2B\cos\omega t\sigma_x = \left[ \begin{array}{cc} \frac{1}{2}A & 2B\cos\omega t \\ 2B\cos\omega t & -\frac{1}{2}A \end{array} \right]. \tag{3.32}$$

The fourier expansion of $\hat{H}$ is

$$\hat{H}(t) = \begin{bmatrix} \frac{1}{2}A & 0 \\ 0 & -\frac{1}{2}A \end{bmatrix} + \begin{bmatrix} 0 & Be^{i\omega t} \\ Be^{i\omega t} & 0 \end{bmatrix} + \begin{bmatrix} 0 & Be^{-i\omega t} \\ Be^{-i\omega t} & 0 \end{bmatrix} \tag{3.33}$$

and

$$\begin{aligned}
\hat{F} &= \hat{H}(t) - i\frac{\partial}{\partial t} \\
&= \frac{1}{2}A\sigma_z + e^{i\omega t}B\sigma_x + e^{-i\omega t}B\sigma_x - i\frac{\partial}{\partial t} \ .
\end{aligned} \tag{3.34}$$

Then, the Floquet Hamiltonian is

$$\hat{H}_F = \frac{1}{2}AI \otimes \sigma_z$$

$$+ B \begin{bmatrix} & \vdots & & & & \\ \cdots & \begin{matrix} 0 & 0 & 0 & 0 & 0 \\ 1 & 0 & 0 & 0 & 0 \\ 0 & 1 & 0 & 0 & 0 \\ 0 & 0 & 1 & 0 & 0 \\ 0 & 0 & 0 & 1 & 0 \end{matrix} & \cdots \\ & \vdots & & & & \end{bmatrix} \otimes \sigma_x + B \begin{bmatrix} & \vdots & & & & \\ \cdots & \begin{matrix} 0 & 1 & 0 & 0 & 0 \\ 0 & 0 & 1 & 0 & 0 \\ 0 & 0 & 0 & 1 & 0 \\ 0 & 0 & 0 & 0 & 1 \\ 0 & 0 & 0 & 0 & 0 \end{matrix} & \cdots \\ & \vdots & & & & \end{bmatrix} \otimes \sigma_x$$

$$- \begin{bmatrix} & \vdots & & & & \\ \cdots & \begin{matrix} 2\omega & 0 & 0 & 0 & 0 \\ 0 & 1\omega & 0 & 0 & 0 \\ 0 & 0 & 0\omega & 0 & 0 \\ 0 & 0 & 0 & -1\omega & 0 \\ 0 & 0 & 0 & 0 & -2\omega \end{matrix} & \cdots \\ & \vdots & & & & \end{bmatrix} \otimes I$$

$$
= \begin{bmatrix}
& \vdots & & \vdots & & \\
\frac{1}{2}A - \omega & 0 & 0 & B & 0 & 0 \\
0 & -\frac{1}{2}A - \omega & B & 0 & 0 & 0 \\
\cdots \quad 0 & B & \frac{1}{2}A + 0\omega & 0 & 0 & B & \cdots \\
\cdots \quad B & 0 & 0 & -\frac{1}{2}A + 0\omega & B & 0 & \cdots \\
0 & 0 & 0 & B & \frac{1}{2}A + \omega & 0 \\
0 & 0 & B & 0 & 0 & -\frac{1}{2}A + \omega \\
& \vdots & & \vdots & &
\end{bmatrix} .
$$

### 3.3.2 Driven oscillators

The Hamiltonian of an oscillator with an external driving $\hat{x}\cos\omega t$ can be written as $(\hbar = 1)$

$$
H(t) = H_0 + 2A\left(\hat{a} + \hat{a}^+\right)\cos\left(\omega t\right) \tag{3.35}
$$

$$
= H_0 + A\left(\hat{a} + \hat{a}^+\right)e^{i\omega t} + A\left(\hat{a} + \hat{a}^+\right)e^{-i\omega t} , \tag{3.36}
$$

where $a$ and $a^+$ are respective the creation and annihilation operators of the system. The corresponding Floquet Hamiltonian is

$$
F = H_0 - i\frac{\partial}{\partial t} + A\left(\hat{a} + \hat{a}^+\right)e^{i\omega t} + A\left(\hat{a} + \hat{a}^+\right)e^{-i\omega t} .
$$

$$
F = \begin{bmatrix}
& \vdots & & & & \\
& 1 & 0 & 0 & 0 & 0 & \\
& 0 & 1 & 0 & 0 & 0 & \\
\cdots & 0 & 0 & 1 & 0 & 0 & \cdots \\
& 0 & 0 & 0 & 1 & 0 & \\
& 0 & 0 & 0 & 0 & 1 & \\
& \vdots & & & &
\end{bmatrix} \otimes H_0 - \omega
\begin{bmatrix}
& \vdots & & & & \\
& 2 & 0 & 0 & 0 & 0 & \\
& 0 & 1 & 0 & 0 & 0 & \\
\cdots & 0 & 0 & 0 & 0 & 0 & \cdots \\
& 0 & 0 & 0 & -1 & 0 & \\
& 0 & 0 & 0 & 0 & -2 & \\
& \vdots & & & &
\end{bmatrix} \otimes I
$$

$$
+ A \begin{bmatrix} & \vdots & & & & \\ & 0 & 0 & 0 & 0 & 0 \\ & 1 & 0 & 0 & 0 & 0 \\ \cdots & 0 & 1 & 0 & 0 & 0 & \cdots \\ & 0 & 0 & 1 & 0 & 0 \\ & 0 & 0 & 0 & 1 & 0 \\ & \vdots & & & & \end{bmatrix} \otimes \left( a + a^+ \right) + A \begin{bmatrix} & \vdots & & & & \\ & 0 & 1 & 0 & 0 & 0 \\ & 0 & 0 & 1 & 0 & 0 \\ \cdots & 0 & 0 & 0 & 1 & 0 & \cdots \\ & 0 & 0 & 0 & 0 & 1 \\ & 0 & 0 & 0 & 0 & 0 \\ & \vdots & & & & \end{bmatrix} \otimes \left( a + a^+ \right)
$$

$$
= \begin{bmatrix} & & & \vdots & & & \\ H_0 - 2\omega & A\left(a+a^+\right) & 0 & 0 & 0 \\ A\left(a+a^+\right) & H_0 - \omega & A\left(a+a^+\right) & 0 & 0 \\ \cdots & 0 & A\left(a+a^+\right) & H_0 & A\left(a+a^+\right) & 0 & \cdots \\ 0 & 0 & A\left(a+a^+\right) & H_0 + \omega & A\left(a+a^+\right) \\ 0 & 0 & 0 & A\left(a+a^+\right) & H_0 + 2\omega \\ & & & \vdots & & & \end{bmatrix} .
$$

Take a driven non-linear oscillator, which will be used in the following section, as an example. The Hamiltonian has the form

$$
H(t) = \frac{\hat{p}^2}{2m} + \frac{m\omega_0^2}{2}\hat{x}^2 + \frac{\alpha}{4}\hat{x}^4 + \hat{x}f\cos\omega t , \tag{3.37}
$$

where $m$ and $\omega_0$ are the mass and the harmonic frequency of the oscillator respectively, and $\alpha$ represents the strength of the non-linearity. Figure 3.1 shows the quasienergy spectrum of Eq. (3.37). Dashed lines show the quasienergy spectrum for a vanishing driving force, and the quasienergy lines cross as the driving frequency increases. When the driving force exists, the quasienergy lines (in solid lines), show anti-crossing behavior. This implies the multiphoton resonance process. In the following chapter, we will discuss this in more details.
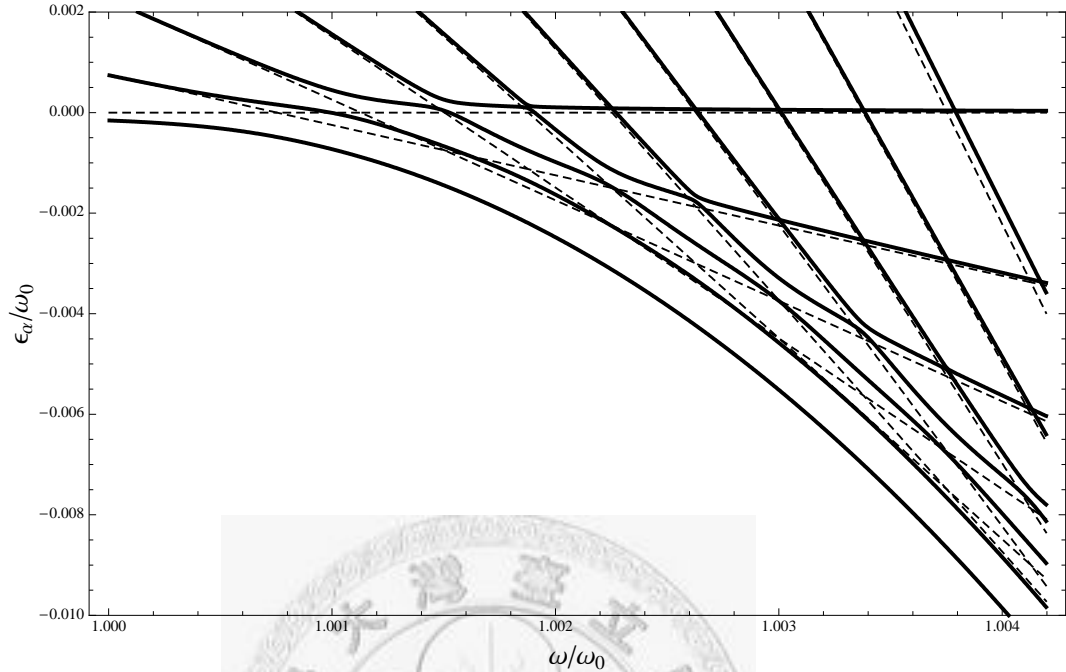
**Figure 3.1** The quasienergy spectrum, $\epsilon_\alpha$ versus $\omega$. Solid lines: $f = 0.001$ and $\alpha = 0.001$. Dashed lines: $f = 0$ and $\alpha = 0.001$.

### 3.3.3 The rotating wave approximation

In this subsection, we introduce a method to reduce the dimension of the Floquet Hamiltonian using the rotating wave approximation. For example, the Hamiltonian of a driven two-level system under the RWA can be written as

$$\hat{H}(t) = \frac{1}{2}A\sigma_z + Be^{i\omega t}\sigma_- + Be^{-i\omega t}\sigma_+ = \begin{bmatrix} \frac{1}{2}A & Be^{-i\omega t} \\ Be^{i\omega t} & -\frac{1}{2}A \end{bmatrix}, \qquad (3.38)$$

and the Floquet Hamiltonian is

$$
\hat{H}_F =
\begin{bmatrix}
 & \vdots & & \vdots & & \\
\frac{1}{2}A - \omega & 0 & 0 & B & 0 & 0 \\
0 & -\frac{1}{2}A - \omega & 0 & 0 & 0 & 0 \\
\cdots \quad 0 & 0 & \frac{1}{2}A + 0\omega & 0 & 0 & B \quad \cdots \\
\cdots \quad B & 0 & 0 & -\frac{1}{2}A + 0\omega & 0 & 0 \quad \cdots \\
0 & 0 & 0 & 0 & \frac{1}{2}A + \omega & 0 \\
0 & 0 & B & 0 & 0 & -\frac{1}{2}A + \omega \\
 & \vdots & & \vdots & &
\end{bmatrix} .
$$

We can find that the state $|\downarrow, n\rangle$ is only involved in $|\uparrow, n+1\rangle$, where $|\downarrow\rangle$ and $|\uparrow\rangle$ are the lower and the higher eigenstate of the two-level system, respectively. In other words, if we rearrange the basis, the Floquet Hamiltonian will be block diagonal. Furthermore, the effective Floquet Hamiltonian for an initial state $|\downarrow, 0\rangle$ is thus only

$$
\begin{bmatrix}
\frac{1}{2}A + \omega & B \\
B & -\frac{1}{2}A
\end{bmatrix} ,
\tag{3.39}
$$

and other states will not couple to it under the RWA. Thus, solving an infinite matrix becomes solving a two-by-two matrix. No matter a driven two-level system or a driven multi-level oscillator, both of their Floquet Hamiltonians can be reduced to smaller ones under the RWA.

## 3.4 Time evolution operators

If we want to evaluate the dynamics of a driven periodic system using the Floquet formalism, the first step is to project an initial state in the Schrödinger picture to the extended Hilbert space. The choice is not unique. Because the condition is that after

we trace over the time domain, probability in the original Hilbert space is conserved. For example, for an initail state in $|\alpha\rangle$ at $t = 0$, the possible choices of the state in the extended Floquet Hilbert space could be

$$|\alpha\rangle \rightarrow |\alpha, 0\rangle \, , \ |\alpha\rangle \rightarrow \frac{1}{\sqrt{2}}[|\alpha, 0\rangle + |\alpha, 1\rangle], \ |\alpha\rangle \rightarrow \frac{1}{\sqrt{2}}[|\alpha, 2\rangle + |\alpha, 1\rangle], \ \text{or} \ ... \, .$$

For convenience, we always choose

$$|\alpha\rangle \rightarrow |\alpha, 0\rangle \ . \tag{3.40}$$

Another important step is projecting final states into a specific state $|\beta\rangle$ to get probability in this state. Obviously, We need to sum all $|\beta, n\rangle$ state in the extended space and add the time evolution $e^{in\omega t}$ back, i.e.

$$\langle\beta| \rightarrow \sum_n \langle\beta n| \, e^{in\omega t} \ . \tag{3.41}$$

The dynamics of the system state is given by Eq. (3.2). With the system being in an initial state $|\alpha\rangle$, the probability amplitude of finding the system in a state $\langle\beta|$ is given by

$$
\begin{aligned}
\langle\beta|\Psi(t)\rangle &= \langle\beta| \sum_\alpha e^{-i\epsilon_\alpha t} |\phi_\alpha(t)\rangle \langle\phi_\alpha(t)|\alpha\rangle \\
&= \sum_n \langle\beta n| \, e^{-i\hat{H}_F t} \sum_\alpha |\phi_\alpha(t)\rangle \langle\phi_\alpha(t)|\alpha 0\rangle \, e^{in\omega t} \\
&= \sum_n \left\langle \beta n \left| e^{-i\hat{H}_F t} \right| \alpha 0 \right\rangle e^{in\omega t} \, ,
\end{aligned}
\tag{3.42}
$$

where the identity property has been used. Now we have the time evolution operator

$$
\begin{aligned}
\hat{U}_{\alpha\beta}(t, t_0) &\equiv \left\langle \beta \left| \hat{U}(t, t_0) \right| \alpha \right\rangle \\
&= \sum_n \left\langle \beta n \left| e^{-i\hat{H}_F(t-t_0)} \right| \alpha 0 \right\rangle e^{in\omega t} \ .
\end{aligned}
\tag{3.43}
$$

## 3.5　Conclusions

In analogy with quasimomenta in the Bloch theory, quasienergies $\epsilon_\alpha$ are defined up to a multiple integer of $\omega$ in the Floquet Hamiltonian. States differing by $e^{in\omega t}$ correspond to the same solution. The Floquet theory makes a Fourier expansion in time domain, and this is in analogy with the Bloch theory in real space domain.

Observing the end of previous section, Eq. (3.43), we can understand that when facing a time-periodic problem, we transfer initial states to an extended Hilbert space, and then the states evolve with the Floquet Hamiltonian as if evolving with a Hamiltonian in a time-independent problem. Finally we transfer the final states back to the original Hilbert space. Thus a time-dependent problem effectively becomes a time-independent problem. Although the matrix $F$ is an infinite dimensional matrix, we can truncate it to particular needed dimensions. The spreading speed in the extended Hilbert space depends on the strength of the driving amplitude.

# Chapter 4

# Quantum dissipation

## 4.1  The Density Matrix

Quantum mechanical state vectors $|\psi\rangle$ convey the total information about a system. If there are two possible states, $|\psi_1\rangle$ and $|\psi_2\rangle$, and they are orthogonal, we may say their superposition

$$|\psi_3\rangle = c_1 |\psi_1\rangle + c_2 |\psi_2\rangle \tag{4.1}$$

present some probability of $|\psi_1\rangle$ and some of $|\psi_2\rangle$. Despite of this, $|\psi_3\rangle$ is still another possible pure state. In other words, a system in $|\psi_3\rangle$ is exactly in the state $|\psi_3\rangle$ not in a mixed state in which the system has a probability $|c_1|^2$ in the $|\psi_1\rangle$ state and a probability $|c_2|^2$ in the $|\psi_2\rangle$ state. In fact there are frequent situations where the state vector is not precisely known. For example, we can't describe a system of interest alone by a state vector, if the system is entangled through interaction with some other systems or its environment. We may write down the state vectors for the total composite system but not for the subsystem we are interested in. There is a famous example, the singlet state of two spin-1/2 particle systems,

$$|\psi\rangle = \frac{1}{\sqrt{2}}[|\uparrow\rangle_1 |\downarrow\rangle_2 - |\downarrow\rangle_1 |\uparrow\rangle_2] \,. \tag{4.2}$$

43

It is impossible to factor this entangled state into a product of states of the two subsystems and, of course, impossible to describes each subsystem separately with a state vector.

### 4.1.1 Pure states and mixed states

Quantum states can be described by state vectors are said to be pure states; if not, are said to be mixed states. Mixed states are described by density matrixes,

$$\hat{\rho} = \sum_i p_i |\psi_i\rangle \langle\psi_i| \ , \tag{4.3}$$

where the sum is over an ensemble (in the sense of statistical mechanics) and $p_i$ is the probability of the system being in the $i$th state $|\psi_i\rangle$ of the ensemble, where $\langle\psi_i|\psi_i\rangle = 1$. Consequently, the probabilities satisfy the relations,

$$0 \le p_i \le 1 \ , \quad \sum_i p_i = 1 \ , \quad \sum_i p_i^2 \le 1 \ . \tag{4.4}$$

Pure states are a special case of mixed states with $p_i = \delta_{ij}$ whose all probability concentrates on one of the ensemble,

$$\hat{\rho} = |\psi_j\rangle \langle\psi_j| \ . \tag{4.5}$$

A density matrix is a sum of the projection operators over the ensemble, weighted with the probability of each member of the ensemble.

Now, we introduce a complete, orthogonal, basis $|\phi_n\rangle$. Then for the $i$th member of the ensemble, we may write

$$|\psi_i\rangle = \sum_n |\phi_n\rangle \langle\phi_n|\psi_i\rangle = \sum_n c_n^{(i)} |\phi_n\rangle \ , \tag{4.6}$$

where $c_n^{(i)} = \langle\phi_n|\psi_i\rangle$. The density matrix is written as

$$\hat{\rho} = \sum_i \sum_{n,n'} p_i c_n^{(i)} c_{n'}^{(i)*} |\phi_n\rangle \langle\phi_{n'}| \ , \tag{4.7}$$

and

$$\mathrm{Tr}\hat{\rho} = 1 \ . \tag{4.8}$$

Note that the number of the summation for $i$ is unlimited, because it sums over the ensemble, but the number of the summation for $n$ depends on the dimension of the system.

It is difficult to distinguish whether a density matrix contains only one projection operator or not. Now, we introduce a useful criteria for pure states and mixed states. For a pure state ,

$$\hat{\rho}^2 = |\psi\rangle \langle\psi|\psi\rangle \langle\psi| = |\psi\rangle \langle\psi| = \hat{\rho} \tag{4.9}$$

and thus

$$\mathrm{Tr}\hat{\rho}^2 = \mathrm{Tr}\hat{\rho} = 1 \ . \tag{4.10}$$

For a mixed states

$$\hat{\rho}^2 = \sum_{i,j} p_i p_j |\psi_i\rangle \langle\psi_i|\psi_j\rangle \langle\psi_j| \tag{4.11}$$

and obviously

$$
\begin{aligned}
\mathrm{Tr}\hat{\rho}^2 &= \sum_n \langle\phi_n| \hat{\rho}^2 |\phi_n\rangle \\
&= \sum_{i,j} p_i p_j |\langle\psi_i|\psi_j\rangle|^2 \\
&\leq \left[\sum_i p_i\right]^2 = 1 \ .
\end{aligned}
\tag{4.12}
$$

### 4.1.2  Ensemble average

For state vectors, the expectation value of some operator $\hat{O}$ is given by

$$\langle \hat{O} \rangle = \langle \psi | \hat{O} | \psi \rangle \ . \tag{4.13}$$

Mixed states is an ensemble of many pure states $|\psi_i\rangle \langle \psi_i|$ with probability $p_i$. So, to evaluate the ensemble average of a mixed state is to sum over all members' expectation values weighted with probabilities $p_i$, which is given by

$$\langle \hat{O} \rangle = \sum_i p_i \langle \psi_i | \hat{O} | \psi_i \rangle \ . \tag{4.14}$$

Formally we may write

$$\langle \hat{O} \rangle = \mathrm{Tr}\left( \hat{\rho} \hat{O} \right) , \tag{4.15}$$

since

$$
\begin{aligned}
\mathrm{Tr}\left( \hat{\rho} \hat{O} \right) &= \sum_n \langle \phi_n | \hat{\rho} \hat{O} | \phi_n \rangle \\
&= \sum_n \sum_i p_i \langle \phi_n | \psi_i \rangle \langle \psi_i | \hat{O} | \phi_n \rangle \\
&= \sum_i \sum_n p_i \langle \psi_i | \hat{O} | \phi_n \rangle \langle \phi_n | \psi_i \rangle \\
&= \sum_i p_i \langle \psi_i | \hat{O} | \psi_i \rangle \ .
\end{aligned}
\tag{4.16}
$$

## 4.2  Derivation of the Master equation

### 4.2.1  Equations of motion of the density matrix of closed systems

For a closed quantum system, the Schrödinger equation describes the dynamics of each possible microstate $|\psi_i\rangle$ with the Hamiltonian $\hat{H}$,

$$\frac{\partial}{\partial t} |\psi_i\rangle = -\frac{i}{\hbar} \hat{H} |\psi_i\rangle \ . \tag{4.17}$$

Taking the time derivative of $\rho$ and then using Eq. (4.17), we have

$$
\begin{aligned}
\dot{\rho} &= \sum_i p_i \left( |\dot{\psi}_i\rangle \langle \psi_i| + |\psi_i\rangle \langle \dot{\psi}_i| \right) \\
&= \sum_i p_i \left( -\frac{i}{\hbar} \hat{H} |\psi_i\rangle \langle \psi_i| + \frac{i}{\hbar} |\psi_i\rangle \langle \psi_i| \hat{H} \right) \\
&= -\frac{i}{\hbar} \left( \hat{H} \sum_i p_i |\psi_i\rangle \langle \psi_i| - \sum_i \mathrm{p}_i |\psi_i\rangle \langle \psi_i| \hat{H} \right) \\
&= -\frac{i}{\hbar} \left( \hat{H} \rho - \rho \hat{H} \right) \\
&= -\frac{i}{\hbar} [\hat{H}, \rho] ,
\end{aligned}
\tag{4.18}
$$

where $p_i$ is probability of the total system in the $i$th state $|\psi_i\rangle$. Eq. (4.18) is called the Liouville-Von Neumann equation of motion for the density matrix, which is only valid for a closed system. We can expect that besides the commutator of the Hamiltonian and the density matrix, other dissipative terms will get involved in a master (evolution) equation of the system density matrix of an open system, a system coupled to other systems or its bath. Usually, we are interested in one subsystem of a closed system or, in other words, a system influenced by its environment. The following sections will discuss how to write down the equation of motion for the subsystem in which we are interested without knowing the details of the rest of the total system.

## 4.2.2 Integro-differential form of the equation of motion for the density matrix

Trying to solve the dynamics of an open system, we divide the total system into two parts; the first part is the subsystem which we are interested in with Hamiltonian $H_S$, and the other part is the rest of the total system, also referred to as a bath, having Hamiltonian $\hat{H}_B$. Since the two subsystems couple to each other, there is also

interaction Hamiltonian $\hat{H}_{SB}$. Then, the total Hamiltonian can be written as

$$\hat{H}(t) = \hat{H}_S + \hat{H}_B + \hat{H}_{SB} \, , \tag{4.19}$$

and the Hilbert space of the total system is defined by

$$\hat{\mathcal{H}} = \hat{\mathcal{H}}_S \otimes \hat{\mathcal{H}}_B \, . \tag{4.20}$$

Because the total world is always a closed system, the total density matrix $\chi(t)$ obeys the Liouville-Von Neumann equation, Eq. (4.18). Thus we obtain

$$\dot{\chi}(t) = -\frac{i}{\hbar}[\hat{H}(t), \chi(t)] \, , \tag{4.21}$$

where $\hat{H}$ is defined by Eq. (4.19). If coupling between the system and the bath is very weak relatively to the rest of the Hamiltonian, it is very suitable to transform the equation into the interaction picture in order to freeze out the time evolution of the density matrix generated by $\hat{H}_B + \hat{H}_S$. This is standard method to freeze out the dominant terms first, and then treat the weak terms as perturbation. Let us define

$$\tilde{\chi}(t) = e^{\frac{i}{\hbar}(\hat{H}_S + \hat{H}_B)t} \chi(t) e^{-\frac{i}{\hbar}(\hat{H}_S + \hat{H}_B)t} \, ,$$
$$\chi(t) = e^{-\frac{i}{\hbar}(\hat{H}_S + \hat{H}_B)t} \tilde{\chi}(t) e^{\frac{i}{\hbar}(\hat{H}_S + \hat{H}_B)t} \, . \tag{4.22}$$

Taking the time derivative and substituting the result into Eq. (4.21), we have

$$\dot{\chi} = -\frac{i}{\hbar}(\hat{H}_S + \hat{H}_B)e^{-\frac{i}{\hbar}(\hat{H}_S + \hat{H}_B)t} \tilde{\chi}(t) e^{\frac{i}{\hbar}(\hat{H}_S + \hat{H}_B)t}$$
$$+ e^{-\frac{i}{\hbar}(\hat{H}_S + \hat{H}_B)t} \dot{\tilde{\chi}}(t) e^{\frac{i}{\hbar}(\hat{H}_S + \hat{H}_B)t}$$
$$+ e^{-\frac{i}{\hbar}(\hat{H}_S + \hat{H}_B)t} \tilde{\chi}(t) \frac{i}{\hbar}(\hat{H}_S + \hat{H}_B) e^{\frac{i}{\hbar}(\hat{H}_S + \hat{H}_B)t}$$
$$= -\frac{i}{\hbar}[\hat{H}_S + \hat{H}_B + \hat{H}_{SB}, \chi(t)]$$
$$= -\frac{i}{\hbar}(\hat{H}_S + \hat{H}_B + \hat{H}_{SB})e^{-\frac{i}{\hbar}(\hat{H}_S + \hat{H}_B)t} \tilde{\chi}(t) e^{\frac{i}{\hbar}(\hat{H}_S + \hat{H}_B)t}$$
$$+ \frac{i}{\hbar} e^{-\frac{i}{\hbar}(\hat{H}_S + \hat{H}_B)t} \tilde{\chi}(t) e^{\frac{i}{\hbar}(\hat{H}_S + \hat{H}_B)t} (\hat{H}_S + \hat{H}_B + \hat{H}_{SB}) \, .$$

Therefore, we obtain

$$e^{-\frac{i}{\hbar}(\hat{H}_S+\hat{H}_B)t}\dot{\tilde{\chi}}(t)e^{\frac{i}{\hbar}(\hat{H}_S+\hat{H}_B)t}$$

$$= -\frac{i}{\hbar}\hat{H}_{SB}e^{-\frac{i}{\hbar}(\hat{H}_S+\hat{H}_B)t}\tilde{\chi}(t)e^{\frac{i}{\hbar}(\hat{H}_S+\hat{H}_B)t} + \frac{i}{\hbar}e^{-\frac{i}{\hbar}(\hat{H}_S+\hat{H}_B)t}\tilde{\chi}(t)e^{\frac{i}{\hbar}(\hat{H}_S+\hat{H}_B)t}\hat{H}_{SB} \ . \quad (4.23)$$

Defining

$$\tilde{H}_{SB}(t) = e^{\frac{i}{\hbar}(\hat{H}_S+\hat{H}_B)t}\hat{H}_{SB}(t)e^{-\frac{i}{\hbar}(\hat{H}_S+\hat{H}_B)t} \ , \quad (4.24)$$

we can rewrite Eq. (4.23) as

$$\dot{\tilde{\chi}}(t) = -\frac{i}{\hbar}\left[e^{\frac{i}{\hbar}(\hat{H}_S+\hat{H}_B)t}\hat{H}_{SB}e^{-\frac{i}{\hbar}(\hat{H}_S+\hat{H}_B)t}\tilde{\chi}(t) - \tilde{\chi}(t)e^{\frac{i}{\hbar}(\hat{H}_S+\hat{H}_B)t}\hat{H}_{SB}e^{-\frac{i}{\hbar}(\hat{H}_S+\hat{H}_B)t}\right]$$

$$= -\frac{i}{\hbar}\left[\tilde{H}_{SB},\tilde{\chi}(t)\right] \ . \quad (4.25)$$

Integrating Eq. (4.25), we get the integral form written as

$$\tilde{\chi}(t) = \tilde{\chi}(0) + \frac{i}{\hbar}\int_0^t dt'\frac{i}{\hbar}\left[\tilde{H}_{SB}(t'),\tilde{\chi}(t')\right] \ , \quad (4.26)$$

and we insert it back into Eq. (4.25) to obtain

$$\dot{\tilde{\chi}}(t) = -\frac{i}{\hbar}\left[\tilde{H}_{SB}(t),\tilde{\chi}(0) + \frac{i}{\hbar}\int_0^t dt'\frac{i}{\hbar}\left[\tilde{H}_{SB}(t'),\tilde{\chi}(t')\right]\right]$$

$$= -\frac{i}{\hbar}\left[\tilde{H}_{SB}(t),\tilde{\chi}(0)\right] - \frac{1}{\hbar^2}\int_0^t dt'\left[\tilde{H}_{SB}(t),\left[\tilde{H}_{SB}(t'),\tilde{\chi}(t')\right]\right] \ . \quad (4.27)$$

Now we define the reduced density matrix of the system as $\rho$ which has the property,

$$\rho(t) = \text{Tr}_{bath}\left[\chi(t)\right] = \text{Tr}_B\left[\chi(t)\right] \ . \quad (4.28)$$

What we want is to obtain the equation which describe the dynamics of the system without the bath and to understand how $\rho(t)$ get involved with the interaction, so we

take the trace over bath variables. At first, we have

$$
\begin{aligned}
\mathrm{Tr}_B[\tilde{\chi}(t)] &= \mathrm{Tr}_B\left[e^{\frac{i}{\hbar}(\hat{H}_S+\hat{H}_B)t}\chi(t)e^{-\frac{i}{\hbar}(\hat{H}_S+\hat{H}_B)t}\right]\\
&= e^{\frac{i}{\hbar}\hat{H}_St}\mathrm{Tr}_B\left[e^{\frac{i}{\hbar}\hat{H}_Bt}\chi(t)e^{-\frac{i}{\hbar}\hat{H}_Bt}\right]e^{-\frac{i}{\hbar}\hat{H}_St}\\
&= e^{\frac{i}{\hbar}\hat{H}_St}\left[\sum_i\langle\phi_i^B|e^{\frac{i}{\hbar}\hat{H}_Bt}\chi(t)e^{-\frac{i}{\hbar}\hat{H}_Bt}|\phi_i^B\rangle\right]e^{-\frac{i}{\hbar}\hat{H}_St}\\
&= e^{\frac{i}{\hbar}\hat{H}_St}\left[\sum_i\langle\phi_i^B|e^{\frac{i}{\hbar}E_i^Bt}\chi(t)e^{-\frac{i}{\hbar}E_i^Bt}|\phi_i^B\rangle\right]e^{-\frac{i}{\hbar}\hat{H}_St}\\
&= e^{\frac{i}{\hbar}\hat{H}_St}\left[\sum_i\langle\phi_i^B|\chi(t)|\phi_i^B\rangle\right]e^{-\frac{i}{\hbar}\hat{H}_St}\\
&= e^{\frac{i}{\hbar}\hat{H}_St}\mathrm{Tr}_B\left[\chi(t)\right]e^{-\frac{i}{\hbar}\hat{H}_St}\\
&= e^{\frac{i}{\hbar}\hat{H}_St}\rho e^{-\frac{i}{\hbar}\hat{H}_St} = \tilde{\rho}(t)\,,
\end{aligned}
\tag{4.29}
$$

where $E_i^B$ and $|\phi_i^B\rangle$ correspond to the eigenvalue and the eigenstate of $\hat{H}_B$, respectively, and $\tilde{\rho}$ is the reduced density matrix of the system in the interaction picture,

$$
\tilde{\rho}(t) = e^{\frac{i}{\hbar}\hat{H}_St}\rho e^{-\frac{i}{\hbar}\hat{H}_St}.
\tag{4.30}
$$

Note that the transformation between $\rho$ and $\tilde{\rho}$ involves only the free system Hamiltonian $\hat{H}_S$. Taking the trace of Eq. (4.27) over the bath degrees of freedom, we have

$$
\begin{aligned}
\dot{\tilde{\rho}}(t) &= \frac{\partial}{\partial t}\mathrm{Tr}_B\left[\tilde{\chi}(t)\right] = \mathrm{Tr}_B\left[\dot{\tilde{\chi}}(t)\right]\\
&= -\frac{i}{\hbar}\mathrm{Tr}_B\left\{[\tilde{H}_{SB}(t),\tilde{\chi}(0)]\right\} - \frac{1}{\hbar^2}\int_0^t \mathrm{d}t'\mathrm{Tr}_B\left\{\left[\tilde{H}_{SB}(t),\left[\tilde{H}_{SB}(t'),\tilde{\chi}(t')\right]\right]\right\}.
\end{aligned}
$$
$$
\tag{4.31}
$$

In order to solve this equation (4.31), we must know the details of the bath since there is the term $\chi$ in it. As a result, it is hard to utilize this equation until some approximation is performed to get rid of the bath. Up to now, Eq. (4.31) is exact without any approximation, and in this form, it is more convenient for us to perform some reasonable approximations on Eq. (4.31) in the following sections.

### 4.2.3 The Born approximation

One can assume that before $t = 0$ there is no interaction and correlation between systems and baths. Then $\tilde{\chi}(0) = \chi(0)$ is separable,

$$\chi(0) = \rho(0) \otimes R_0 , \tag{4.32}$$

where $R_0$ is an initial reservoir density operator. If the bath are very big and the coupling $\hat{H}_{SB}$ is very weak, the feedback from the system to the bath can be neglected. So when $t > 0$ the bath still stays in the initial density operator,

$$\tilde{\chi}(t) = \tilde{\rho}(t) \otimes R_0 , \tag{4.33}$$

called the Born approximation. Furthermore, we usually assume that the bath stays in thermal equilibrium,

$$R_0 = \frac{e^{-\beta \hat{H}_B}}{\text{Tr} e^{-\beta \hat{H}_B}} . \tag{4.34}$$

With Eq. (4.31), (4.32) and (4.33), a closed integro-diffrential equation for the reduced density matrix of the system in the interaction picture is obtained,

$$\dot{\tilde{\rho}}(t) = -\frac{i}{\hbar} \text{Tr}_B \left\{ \left[ \tilde{H}_{SB}(t), \tilde{\rho}(0) \otimes R_0 \right] \right\}$$
$$- \frac{1}{\hbar^2} \int_0^t dt' \text{Tr}_B \left\{ \left[ \tilde{H}_{SB}(t), \left[ \tilde{H}_{SB}(t'), \tilde{\rho}(t') \otimes R_0 \right] \right] \right\} . \tag{4.35}$$

### 4.2.4 The Markovian approximation and bath correlation functions

Obviously, Eq. (4.35) is a complicated equation. The term $\tilde{\rho}(t')$ inside the integral equation reveals that the future not only depends on its present state but also influenced by its past history. In the following, another important approximation, the Markovian approximation, will be introduced.

Denoting system operators by $\hat{S}_k$ and bath operators by $\hat{B}_k$, the most general form of coupling $\hat{H}_{SB}$ is

$$\hat{H}_{SB} = \sum_k \hat{S}_k \otimes \hat{B}_k . \tag{4.36}$$

Inserting Eq. (4.36) into Eq. (4.35), we have

$$\dot{\tilde{\rho}}(t) = -\frac{i}{\hbar} \sum_k \mathrm{Tr}_B \left\{ [\tilde{S}_k(t) \otimes \tilde{B}_k(t), \tilde{\rho}(0) \otimes R_0] \right\}$$
$$- \frac{1}{\hbar^2} \int_0^t \mathrm{d}t' \sum_{kl} \mathrm{Tr}_B \left\{ \left[ \tilde{S}_k(t) \otimes \tilde{B}_k(t), \left[ \tilde{S}_l(t') \otimes \tilde{B}_k(t'), \tilde{\rho}(t') \otimes R_0 \right] \right] \right\} . \tag{4.37}$$

It is usually assumed that the reservoir operators coupling to the system have zero mean in the thermal equilibrium state $R_0$,

$$\mathrm{Tr} \left[ \tilde{B}_k(t) R_0 \right] = 0 . \tag{4.38}$$

This is true for thermal equilibrium bath. So, the first term on the right side of Eq. (4.35) vanishes. We will also encounter the bath correlation functions,

$$C_{kl}(t - t') \equiv \mathrm{Tr}_B \left[ \tilde{B}_k(t) \tilde{B}_l(t') R_0 \right] , \tag{4.39}$$

in the second term. Those mean two different time average and will approach to a delta function if the decay rate of the bath, comparing with the dynamics of the system, is relatively fast,

$$C_{kl} \propto \delta(t - t') . \tag{4.40}$$

Under this condition, $\tilde{\rho}(t')$ can be replaced by $\tilde{\rho}(t)$, called the Markovian approximation. This means that because the decay of the bath is very fast, the history of the system can't be memorized in the bath. Therefore, the future of the system just depends on its present state. Besides, because the bath correlation function is strongly peaked around $t - t' = 0$, the integral over $t'$ can be carried out to $t = \infty$. With above assumptions, we get the Born-Markov master equation in the interaction

picture from Eq. (4.35),

$$\dot{\rho}(t) = -\frac{1}{\hbar^2} \int_0^\infty dt' \text{Tr}_B \left\{ \left[ \tilde{H}_{SB}(t), \left[ \tilde{H}_{SB}(t'), \tilde{\rho}(t) \otimes R_0 \right] \right] \right\} . \tag{4.41}$$

Now we try to transform it back into the Schrödinger picture by using the following relation

$$\tilde{\rho}(t) \equiv e^{\frac{i}{\hbar}\hat{H}_S t} \rho e^{-\frac{i}{\hbar}\hat{H}_S t}$$

$$\Rightarrow \quad \frac{d}{dt}\tilde{\rho}(t) = \frac{i}{\hbar} \left[ \hat{H}_S, \tilde{\rho}(t) \right] + e^{\frac{i}{\hbar}\hat{H}_S t} \frac{d}{dt} \rho e^{-\frac{i}{\hbar}\hat{H}_S t}$$

$$\Rightarrow \quad \frac{d}{dt}\rho(t) = -\frac{i}{\hbar} \left[ \hat{H}_S, \rho(t) \right] + e^{-\frac{i}{\hbar}\hat{H}_S t} \frac{d}{dt} \tilde{\rho} e^{\frac{i}{\hbar}\hat{H}_S t} , \tag{4.42}$$

The Born-Markov master equation in the Schrödinger picture is given by

$$\dot{\rho}(t) = -\frac{i}{\hbar} \left[ \hat{H}_S, \rho(t) \right] - \frac{1}{\hbar^2} \int_0^\infty dt' \text{Tr}_B \left\{ \left[ \hat{H}_{SB}, \left[ \tilde{H}_{SB}(t' - t), \rho(t) \otimes R_0 \right] \right] \right\} . \tag{4.43}$$

## 4.3 Master equations of driven systems

### 4.3.1 The derivation of master equations

In the previous section, the Hamiltonian of the system is time-independent in the Schrödinger picture. In this section, a damped system with driving will be discussed. The derivation of the master equation in the interaction picture is analogous to that of a time-independent system. The only difference is that the unitary operator transforming Liouville-Von Neumann equations (4.21) from the Schrödinger picture into the interaction picture is defined by

$$U_0(t, t') = \mathcal{T} exp \left( -\frac{i}{\hbar} \int_{t'}^t dt'' [\hat{H}_S(t'') + \hat{H}_B] \right) , \tag{4.44}$$

and operators in the interaction picture are defined by

$$\tilde{O}(t, t') = U_0^+(t, t') \hat{O} U_0(t, t') , \tag{4.45}$$

where $\mathcal{T}$ is Wick's time-ordering operator. Making the change of variable for convenience,

$$\tau = t - t' \, , \tag{4.46}$$

we can restate Eq. (4.41) as

$$\dot{\tilde{\rho}}(t) = -\frac{1}{\hbar^2} \int_0^\infty \mathrm{d}\tau \, \mathrm{Tr}_B \left\{ \left[ \tilde{H}_{SB}(t,0), \left[ \tilde{H}_{SB}(t-\tau,0), \tilde{\rho}(t) \otimes R_0 \right] \right] \right\} \, , \tag{4.47}$$

and by using

$$\dot{\rho}(t) = -\frac{i}{\hbar} \left[ \hat{H}_S(t), \rho(t) \right] + U_0(t,0) \dot{\tilde{\rho}}(t) U_0^+(t,0) \, , \tag{4.48}$$

the master equation of a time-dependent system in the Schrödinger picture is given by

$$
\begin{aligned}
\dot{\rho}(t) = &-\frac{i}{\hbar} \left[ \hat{H}_S(t), \rho(t) \right] \\
&-\frac{1}{\hbar^2} \int_0^\infty \mathrm{d}\tau \, \mathrm{Tr}_B \left\{ U_0(t,0) \left[ \tilde{H}_{SB}(t,0), \left[ \tilde{H}_{SB}(t-\tau,0), \tilde{\rho}(t) \otimes R_0 \right] \right] U_0^+(t,0) \right\} \\
= &-\frac{i}{\hbar} \left[ \hat{H}_S(t), \rho(t) \right] -\frac{1}{\hbar^2} \int_0^\infty \mathrm{d}\tau \, \mathrm{Tr}_B \left\{ \left[ \hat{H}_{SB}, \left[ \tilde{H}_{SB}(t-\tau,t), \rho(t) \otimes R_0 \right] \right] \right\} \, .
\end{aligned}
\tag{4.49}
$$

Note that the term $\tilde{H}_{SB}(t-\tau,t)$ in Eq. (4.49) is different form the term $\tilde{H}_{SB}(t'-t)$ in Eq. (4.43). In a time-independent system, operators in the interaction picture $\tilde{H}_{SB}(t'-t)$ can be easily transformed back into the Schrödinger picture by using the commutator relation and we just focus on how big the time difference interval is. But it is difficult to transform operators in a time-dependent system with the time-ordering operator and we must be very careful about when the time interval starts and when it ends. For example, $\tilde{H}_{SB}(t-\tau,t)$ is different from $\tilde{H}_{SB}(-\tau,0)$.

## 4.3.2   Microscopic models of dissipation

Now an explicit model is adopted [27]. The total Hamiltonian in the composite Hilbert space is

$$\hat{H}(t) = \hat{H}_S(t) + \hat{H}_{SB} + \hat{H}_B \ , \tag{4.50}$$

where the bath,

$$\hat{H}_B = \sum_{\nu=1}^{N} \left( \frac{\hat{p}_\nu^2}{2m_\nu} + \frac{m_\nu}{2}\omega_\nu^2 \hat{x}_\nu^2 \right) \ , \tag{4.51}$$

is modeled as a collection of $N$ oscillators with masses $m_\nu$, frequencies $\omega_\nu$, momenta operators $\hat{p}_\nu$, and position operators $x_\nu$. The system is coupled to the bath bilinearly via

$$\hat{H}_{SB} = -\hat{x} \sum_{\nu=1}^{N} g_\nu \hat{x}_\nu + \hat{x}^2 \sum_{\nu=1}^{N} \frac{g_\nu^2}{2m_\nu \omega_\nu^2} \ , \tag{4.52}$$

where $g_\nu$ is the coupling strength of the $\nu$th oscillator coupled to the system. The second term of Eq. (4.52) is just to cancel the renormalization energy due to the coupling to the bath, and is neglected in the following. The bath is fully characterized by the spectral density of the coupling energy,

$$I(\omega) = \pi \sum_{v=1}^{N} \frac{\hat{g}_v^2}{2m_\nu \omega_\nu} \delta\left(\omega - \omega_\nu\right) \ . \tag{4.53}$$

Then, we substitute Eq. (4.51) and (4.52) into Eq. (4.49). The trace of double commutator inside the integration of Eq. (4.49) is

$$\mathrm{Tr}_B\left\{ \left[ \hat{H}_{SB}, \left[ \tilde{H}_{SB}(t-\tau, t), \rho(t) \otimes R_0 \right] \right] \right\} =$$

$$Tr_B\left\{ \hat{H}_{SB}\tilde{H}_{SB}(t-\tau,t)\rho(t) \otimes R_0 \right\} - Tr_B\left\{ \hat{H}_{SB}\rho(t) \otimes R_0 \tilde{H}_{SB}(t-\tau,t) \right\}$$

$$-Tr_B\left\{ \tilde{H}_{SB}(t-\tau,t)\rho(t) \otimes R_0 \hat{H}_{SB} \right\} + Tr_B\left\{ \rho(t) \otimes R_0 \tilde{H}_{SB}(t-\tau,t)\hat{H}_{SB} \right\} \ . \tag{4.54}$$

We deal with each term separately. The first term of Eq. (4.54) is

$$
Tr_B\left\{\hat{H}_{SB}\tilde{H}_{SB}(t-\tau,t)\rho(t)\otimes R_0\right\}
$$

$$
= Tr_B\left\{\left[-\hat{x}\sum_{\nu=1}^{N}g_\nu\hat{x}_\nu\right]\left[-\tilde{x}(t-\tau,t)\sum_{\mu=1}^{N}g_\mu\tilde{x}_\mu(t-\tau,t)\right]\rho(t)\otimes R_0\right\}
$$

$$
= Tr_B\left\{\hat{x}\tilde{x}(t-\tau,t)\sum_{\nu\mu=1}^{N}g_\nu g_\mu\hat{x}_\nu\tilde{x}_\mu(t-\tau,t)\rho(t)\otimes R_0\right\}
$$

$$
= \hat{x}\tilde{x}(t-\tau,t)\rho(t)\sum_{\nu\mu=1}^{N}Tr_B\left\{g_\nu g_\mu\hat{x}_\nu\tilde{x}_\mu(t-\tau,t)R_0\right\}
$$

$$
= \hat{x}\tilde{x}(t-\tau,t)\rho(t)\sum_{\nu=1}^{N}Tr_B\left\{g_\nu^2\hat{x}_\nu\tilde{x}_\nu(t-\tau,t)R_0\right\}\,, \tag{4.55}
$$

where $Tr_B\{\hat{x}_\nu\hat{x}_\mu R_0\} = 0$ if $\nu \neq \mu$ is used. Transforming position operators of the bath into creation and annihilation operators $a_\nu^+$ and $a_\nu$, we have

$$
Tr_B\left\{\hat{H}_{SB}\tilde{H}_{SB}(t-\tau,t)\rho(t)\otimes R_0\right\}
$$

$$
= \hat{x}\tilde{x}(t-\tau,t)\rho(t)\sum_{\nu=1}^{N}g_\nu^2\frac{\hbar}{2m_\nu\omega_\nu}Tr_B\left\{\left(\hat{a}_\nu+\hat{a}_\nu^+\right)\left(\tilde{a}_\nu(t-\tau,t)+\tilde{a}_\nu^+(t-\tau,t)\right)R_0\right\}\,,
$$

$$
\tag{4.56}
$$

and from Eq. (4.51), creation and annihilation operators in the interaction picture are

$$
\tilde{a}_\nu(t-\tau,t) = U_0^+(t-\tau,t)\hat{a}_\nu U_0(t-\tau,t) = e^{i\omega_\nu\hat{a}_\nu^+\hat{a}_\nu(-\tau)}\hat{a}_\nu e^{-i\omega_\nu\hat{a}_\nu^+\hat{a}_\nu(-\tau)} = \hat{a}_\nu e^{i\omega_\nu\tau}\,,
$$

$$
\tilde{a}_\nu^+(t-\tau,t) = U_0^+(t-\tau,t)\hat{a}_\nu^+ U_0(t-\tau,t) = e^{i\omega_\nu\hat{a}_\nu^+\hat{a}_\nu(-\tau)}\hat{a}_\nu^+ e^{-i\omega_\nu\hat{a}_\nu^+\hat{a}_\nu(-\tau)} = \hat{a}_\nu^+ e^{i\omega_\nu\tau}\,.
$$

$$
\tag{4.57}
$$

Then Eq. (4.56) becomes

$$
Tr_B\left\{\hat{H}_{SB}\tilde{H}_{SB}(t-\tau,t)\rho(t)\otimes R_0\right\} =
$$

$$
\hat{x}\tilde{x}(t-\tau,t)\rho(t)\sum_{\nu=1}^{N}g_\nu^2\frac{\hbar}{2m_\nu\omega_\nu}Tr_B\left\{\hat{a}_\nu\hat{a}_\nu^+ e^{-i\omega_\nu\tau}R_0 + \hat{a}_\nu^+\hat{a}_\nu e^{i\omega_\nu\tau}R_0\right\}\,, \tag{4.58}
$$

where the properties have been used, $Tr_B \{\hat{a}\hat{a}R_0\} = 0$ and $Tr_B \{\hat{a}^+\hat{a}^+R_0\} = 0$.

With the mean photon number for an oscillator with frequency $\omega_\nu$ in thermal equilibrium at temperature $T$,

$$\bar{n}_\nu \equiv Tr_B \left\{\hat{a}_\nu^+\hat{a}_\nu R_0\right\} = \frac{e^{-\beta\hbar\omega_\nu}}{1 - e^{-\beta\hbar\omega_\nu}} \ , \tag{4.59}$$

we get

$$Tr_B \left\{\hat{H}_{SB}\tilde{H}_{SB}(t - \tau, t)\rho(t) \otimes R_0\right\} =$$
$$\hat{x}\tilde{x}(t - \tau, t)\rho(t) \sum_{\nu=1}^{N} g_\nu^2 \frac{\hbar}{2m_\nu\omega_\nu} \left(\frac{\coth\frac{\beta\hbar\omega_\nu+1}{2}}{2}e^{-i\omega_\nu\tau} + \frac{\coth\frac{\beta\hbar\omega_\nu-1}{2}}{2}e^{i\omega_\nu\tau}\right) . \tag{4.60}$$

Likewise, the second term, the third term and the fourth term of Eq. (4.54) are

$$Tr_B \left\{\hat{H}_{SB}\rho(t) \otimes R_0\tilde{H}_{SB}(t - \tau, t)\right\} =$$
$$\hat{x}\rho(t)\tilde{x}(t - \tau, t) \sum_{\nu=1}^{N} g_\nu^2 \frac{\hbar}{2m_\nu\omega_\nu} \left(\frac{\coth\frac{\beta\hbar\omega_\nu+1}{2}}{2}e^{i\omega_\nu\tau} + \frac{\coth\frac{\beta\hbar\omega_\nu-1}{2}}{2}e^{-i\omega_\nu\tau}\right) , \tag{4.61}$$

$$Tr_B \left\{\tilde{H}_{SB}(t - \tau, t)\rho(t) \otimes R_0\hat{H}_{SB}\right\} =$$
$$\tilde{x}(t - \tau, t)\rho(t)\hat{x} \sum_{\nu=1}^{N} g_\nu^2 \frac{\hbar}{2m_\nu\omega_\nu} \left(\frac{\coth\frac{\beta\hbar\omega_\nu-1}{2}}{2}e^{i\omega_\nu\tau} + \frac{\coth\frac{\beta\hbar\omega_\nu+1}{2}}{2}e^{-i\omega_\nu\tau}\right) , \tag{4.62}$$

$$Tr_B \left\{\rho(t) \otimes R_0\tilde{H}_{SB}(t - \tau, t)\hat{H}_{SB}\right\} =$$
$$\rho(t)\tilde{x}(t - \tau, t)\hat{x} \sum_{\nu=1}^{N} g_\nu^2 \frac{\hbar}{2m_\nu\omega_\nu} \left(\frac{\coth\frac{\beta\hbar\omega_\nu+1}{2}}{2}e^{i\omega_\nu\tau} + \frac{\coth\frac{\beta\hbar\omega_\nu-1}{2}}{2}e^{-i\omega_\nu\tau}\right) . \tag{4.63}$$

With Eq. (4.60)–(4.63) and Eq. (4.49), the master equation is

$$
\dot{\rho}(t) = -\frac{i}{\hbar}\left[\hat{H}_S(t), \rho(t)\right] - \frac{1}{\hbar^2}\int_0^\infty \mathrm{d}\tau \sum_{\nu=1}^N g_\nu^2 \frac{\hbar}{2m_\nu\omega_\nu}\times
$$
$$
\left[\hat{x}\tilde{x}(t-\tau,t)\rho(t)\left(\coth\frac{\beta\hbar\omega_\nu}{2}\cos\omega_\nu\tau - i\sin\omega_\nu\tau\right)\right.
$$
$$
+ \hat{x}\rho(t)\tilde{x}(t-\tau,t)\left(-\coth\frac{\beta\hbar\omega_\nu}{2}\cos\omega_\nu\tau - i\sin\omega_\nu\tau\right)
$$
$$
+ \tilde{x}(t-\tau,t)\rho(t)\hat{x}\left(-\coth\frac{\beta\hbar\omega_\nu}{2}\cos\omega_\nu\tau + i\sin\omega_\nu\tau\right)
$$
$$
\left.+ \rho(t)\tilde{x}(t-\tau,t)\hat{x}\left(-\coth\frac{\beta\hbar\omega_\nu}{2}\cos\omega_\nu\tau + i\sin\omega_\nu\tau\right)\right] . \tag{4.64}
$$

This can be further re-arranged into

$$
\dot{\rho}(t) = -\frac{i}{\hbar}\left[\hat{H}_S(t), \rho(t)\right] - \frac{1}{\hbar^2}\int_0^\infty \mathrm{d}\tau \sum_{\nu=1}^N g_\nu^2\times
$$
$$
\left\{S_\nu(\tau)\left[\hat{x}, [\tilde{x}(t-\tau,t), \rho(t)]\right] + iA_\nu(\tau)\left[\hat{x}, [\tilde{x}(t-\tau,t), \rho(t)]_+\right]\right\} , \tag{4.65}
$$

where $[A, B]_+ = AB + BA$, and

$$
S_\nu(t) = \frac{\hbar}{2m_\nu\omega_\nu}\coth\left(\frac{\hbar\omega_\nu}{2k_BT}\right)\cos\omega_\nu , \tag{4.66}
$$

$$
A_\nu(t) = -\frac{\hbar}{2m_\nu\omega_\nu}\sin\omega_\nu t , \tag{4.67}
$$

are, respectively, the symmetrically ordered and antisymmetrically ordered correlation functions of the bath oscillator $\nu$.

# Chapter 5

# The quantum Duffing oscillator

The Duffing oscillator is a very well-known non-linear oscillator in classical physics [appendix A]. The bistable property is very sensitive to the driving frequency, forming a very cusior ingredient for implementing a device which detects the states of qubits. In this chapter, we introduce the Floquet master equation [27–29] for solving the dynamics of the quantum Duffing oscillator and some simulation results are presented.

## 5.1   Hamiltonian of quantum Duffing oscillator

Both the SQUID and the Josephson junciton presented before have non-linear properties. Their dynamics can be described by a quantum Duffing oscillator model. The Hamiltonian of the quantum Duffing oscillator model is

$$\hat{H}_S = \frac{\hat{p}^2}{2m} + \frac{m\omega_0^2}{2}\hat{x}^2 + \frac{\alpha}{4}\hat{x}^4 + \hat{x}f\cos(\omega_{ex}t) \,, \tag{5.1}$$

where $m$ and $\omega_0$ are the mass and the nature frequency of the oscillator, respectively, $\alpha$ gives the strength of the non-linearity, and $f$ and $\omega$ denote the amplitude and the frequency of the external force. In our discussion, the parameter $\alpha$ is bigger than zero and the potential is single-well.

## 5.2 The Floquet-Born-Markovian master equation

A master equation describes an evolution equation of an quantum open system, and the Floquet formalism is a powerful tool to investigate the dynamical behavior of a driven periodic system. In this section, a technique to combine the master equation with the Floquet formalism, called the Floquet master equation, will be introduced. The Floquet master equation is a master equation using Floquet states as the basis states. This treatment is appropriate for driven periodic quantum open system.

### 5.2.1 The driven weak-coupling master equation

We start from the expression of a master equation in the weak-coupling limit,

$$
\begin{aligned}
\dot{\rho}(t) & = -\frac{i}{\hbar}[\hat{H}_s(t), \rho(t)] + \frac{1}{\pi\hbar}\int_{-\infty}^{\infty}d\omega I(\omega)n_{th}(\omega) \\
& \times \int_0^{\infty}d\tau e^{i\omega\tau}[\tilde{x}(t-\tau, t)\rho(t), \hat{x}] + H.c. \;,
\end{aligned}
\tag{5.2}
$$

and assume an Ohmic spectral density with an exponential cutoff at $\omega_c$ for the bath as

$$
I(\omega) = \pi\sum_{v=1}^{N}\frac{\hat{g}_v^2}{2m_\nu\omega_\nu}\delta(\omega - \omega_\nu) = m\gamma\omega e^{-\omega/\omega_c} \;,
\tag{5.3}
$$

where $\gamma$ is the damping constant. One can always find $\tilde{x}(t-\tau, t)$ in a driven master equation, as

$$
\tilde{x}(t, t') = U_0^+(t, t')\hat{x}U_0(t, t') \;,
\tag{5.4}
$$

$$
U_0(t, t') = \mathcal{T}exp\left(-\frac{i}{\hbar}\int_{t'}^{t}dt''[\hat{H}_S(t'') + \hat{H}_B]\right) \;.
\tag{5.5}
$$

The time-ordering operator $\mathcal{T}$ makes the integration almost impossible to be solved numerically. However, S. Kohler proposed an idea of combining the master equation approach with the Floquet Formalism. Choosing the Floquet states as the basis states [27], and using the fact that the Floquet states of the undamped central system

solve the Schrödinger equation, one can simplify the driven periodic master equation.

### 5.2.2 Complete set property of Floquet states

There are infinite numbers of Floquet states, because the Floquet formalism projects a real Hilbert space $R$ to a bigger one $T \otimes R$. Besides, if $|\phi_\alpha(t)\rangle$ is an eigenstate of the Floquet Hamiltonian, $e^{in\omega_{ex}t}|\phi_\alpha(t)\rangle$ with any integer number $n$ is an eigenstate too. However, they correspond to the same physical state in the Schrödinger picture. Like the Bloch theory, we just need the states in one of "Brillouin zone" in the time domain and a complete set basis contains $N$ states, where $N$ is the dimension of the original Hilbert space. A complete set of Floquet states contains the identity property in the Hilbert space $R$,

$$\sum_{\alpha}^{N} |\phi_\alpha(t)\rangle \langle \phi_\alpha(t)| = I_R . \tag{5.6}$$

Note that the choice is not unique. The basis always can be selected in another Brillouin zone, or even select them in many Brillouin zones at the same time.

### 5.2.3 The Floquet master equation

Now, we represent the density matrix and position operator in the floquet picture,

$$\rho_{\alpha\beta}(t) \equiv \langle \phi_\alpha(t)|\rho(t)|\phi_\beta(t)\rangle , \tag{5.7}$$

$$X_{\alpha\beta}(t) \equiv \langle \phi_\alpha(t)|\hat{x}|\phi_\beta(t)\rangle = \sum_n e^{-in\omega_{ex}t} X_{\alpha\beta,n} . \tag{5.8}$$

$X_{\alpha\beta,n}$ is the Fourier component of $\hat{x}$ in floquet picture and is given by

$$X_{\alpha\beta,n} = \frac{1}{T_{\omega_{ex}}} \int_0^T \mathrm{d}t e^{in\omega_{ex}t} \langle \phi_\alpha(t)|\hat{x}(t)|\phi_\beta(t)\rangle . \tag{5.9}$$

Although the time-ordering operator seems like a trouble problem, fortunately, $U_0(t, t')$ is the time evolution operator of QES, $U_0(t - \tau, t) |\phi_\alpha(t)\rangle = e^{i\epsilon_\alpha \tau/\hbar} |\phi_\alpha(t - \tau)\rangle$. Therefore, we have

$$
\begin{aligned}
\langle \phi_\alpha(t) | \tilde{x}(t - \tau, t) | \phi_\beta(t) \rangle &= \langle \phi_\alpha(t) | U_0^+(t - \tau, t) \hat{x} U_0(t - \tau, t) | \phi_\beta(t) \rangle \\
&= e^{-i(\epsilon_\alpha - \epsilon_\beta)\tau/\hbar} \langle \phi_\alpha(t - \tau) | \hat{x} | \phi_\beta(t - \tau) \rangle \\
&= e^{-i(\epsilon_\alpha - \epsilon_\beta)\tau/\hbar} X_{\alpha\beta}(t - \tau) .
\end{aligned}
\tag{5.10}
$$

We also need

$$
\begin{aligned}
\dot{\rho}_{\alpha\beta}(t) &= \frac{\mathrm{d}}{\mathrm{d}t} \left[ \langle \phi_\alpha(t) | \rho(t) | \phi_\beta(t) \rangle \right] \\
&= \frac{\mathrm{d}}{\mathrm{d}t} \left[ \langle \phi_\alpha(t) | \right] \rho(t) | \phi_\beta(t) \rangle + \langle \phi_\alpha(t) | \rho(t) \frac{\mathrm{d}}{\mathrm{d}t} \left[ | \phi_\beta(t) \rangle \right] \\
&\quad + \langle \phi_\alpha(t) | \dot{\rho}(t) | \phi_\beta(t) \rangle ,
\end{aligned}
\tag{5.11}
$$

and the Floquet properties,

$$
\left[ H_S(t) - i\hbar \frac{\mathrm{d}}{\mathrm{d}t} \right] |\phi_\alpha(t)\rangle = \epsilon_\alpha |\phi_\alpha(t)\rangle .
\tag{5.12}
$$

Using Eqs. (5.2), (5.7), (5.8), and (5.10)−(5.12), we obtain

$$
\begin{aligned}
\dot{\rho}_{\alpha\beta}(t) &= -\frac{i}{\hbar}(\epsilon_\alpha - \epsilon_\beta)\rho_{\alpha\beta}(t) + \frac{1}{\pi\hbar} \int_{-\infty}^{\infty} d\omega I(\omega) n_{th}(\omega) \int_0^{\infty} d\tau e^{i\omega\tau} \\
&\quad \times \sum_{\alpha'\beta'} \left\{ e^{-(\epsilon_\alpha - \epsilon_{\alpha'})\tau/\hbar} X_{\alpha\alpha'}(t - \tau) \rho_{\alpha'\beta'}(t) X_{\beta'\beta}(t) \right. \\
&\quad \left. - e^{-(\epsilon_{\alpha'} - \epsilon_{\beta'})\tau/\hbar} X_{\alpha\beta'}(t) X_{\beta'\alpha'}(t - \tau) \rho_{\alpha'\beta}(t) \right\} + H.c. .
\end{aligned}
\tag{5.13}
$$

With the Fourier expansion, Eq. (5.8), we then have

$$
\begin{aligned}
\dot{\rho}_{\alpha\beta}(t) &= -\frac{i}{\hbar}(\epsilon_\alpha - \epsilon_\beta)\rho_{\alpha\beta}(t) + \frac{1}{\pi\hbar} \int_{-\infty}^{\infty} d\omega I(\omega) n_{th}(\omega) \int_0^{\infty} d\tau e^{i\omega\tau} \\
&\quad \times \sum_{\alpha'\beta'} \sum_{nn'} e^{-i(n+n')\omega_{ext}t} \left\{ e^{-i(\Delta_{\alpha\alpha',-n})\tau/\hbar} X_{\alpha\alpha',n} \rho_{\alpha'\beta'}(t) X_{\beta'\beta,n'} \right. \\
&\quad \left. - e^{-i(\Delta_{\alpha'\beta',-n'})\tau/\hbar} X_{\alpha\beta',n} X_{\beta'\alpha',n'} \rho_{\alpha'\beta}(t) \right\} + H.c. ,
\end{aligned}
\tag{5.14}
$$

where $\Delta_{\alpha\beta,n} = \epsilon_\alpha - \epsilon_\beta + n\hbar\omega_{ex}$. Using the identity $\int_0^\infty d\tau e^{i\omega\tau} = \pi\delta(w) + P(i/\omega)$, we arrive at the explicit equation of motion. Here we neglect the principal part.

$$\dot{\rho}_{\alpha\beta} = -\frac{i}{\hbar}(\epsilon_\alpha - \epsilon_\beta)\rho_{\alpha\beta}(t)$$
$$+ \frac{1}{\hbar}\sum_{\alpha'\beta'}\sum_{nn'} e^{-i(n+n')\omega_{ex}t}\{N_{\alpha\alpha',-n}X_{\alpha\alpha',n}\rho_{\alpha'\beta'}X_{\beta'\beta,n'}$$
$$- N_{\beta'\alpha',-n'}X_{\alpha\beta',n}X_{\beta'\alpha',n'}\rho_{\alpha'\beta} + N_{\beta\beta',n'}X_{\alpha\alpha',n}\rho_{\alpha'\beta'}X_{\beta'\beta,n'}$$
$$- N_{\alpha'\beta',n'}\rho_{\alpha\beta'}X_{\beta'\alpha',n'}X_{\alpha'\beta,n}\} , \tag{5.15}$$

where $N_{\alpha\beta,n} \equiv I\left(\Delta_{\alpha\beta,n}/\hbar\right)n_{th}\left(\Delta_{\alpha\beta,n}/\hbar\right)$.

## 5.2.4 The rotating wave approximation

We have derived the master equation using the Floquet states as the basis, but there is another difficulty. There are functions of time inside. This makes the calculation hard. For the purpose to create a time-independent master equation, we perform rotating-wave approximation here. In Eq. (5.16), $e^{-i(n+n')\omega_{ex}t}$ doesn't vanish only if $n = n'$, yielding

$$\dot{\rho}_{\alpha\beta} = -\frac{i}{\hbar}(\epsilon_\alpha - \epsilon_\beta)\rho_{\alpha\beta}(t) + \frac{1}{\hbar}\sum_{\alpha'\beta'}\sum_n \{N_{\alpha\alpha',-n}X_{\alpha\alpha',n}\rho_{\alpha'\beta'}X_{\beta'\beta,-n}$$
$$- N_{\beta'\alpha',-n}X_{\alpha\beta',-n}X_{\beta'\alpha',n}\rho_{\alpha'\beta} + N_{\beta\beta',-n}X_{\alpha\alpha',n}\rho_{\alpha'\beta'}X_{\beta'\beta,-n}$$
$$- N_{\alpha'\beta',-n}\rho_{\alpha\beta'}X_{\beta'\alpha',-n}X_{\alpha'\beta,n}\} . \tag{5.16}$$

Thus, a time-independent master equation appears.

## 5.2.5 Dynamics of the quantum Duffing oscillator

The most general form of mapping from matrix to matrix is

$$A_{\alpha\beta} = \mathcal{M}_{\alpha\beta\alpha'\beta'}B_{\alpha'\beta'} \tag{5.17}$$

Because $\mathcal{M}$ maps operator $B$ to operator $A$, $\mathcal{M}$ is called a superoperator.

With the help of delta functions, Eq. (5.16) can be rewritten into the following form,

$$\dot{\rho}_{\alpha\beta}(t) = \sum_{\alpha'\beta'} \mathcal{M}_{\alpha\beta,\alpha'\beta'} \rho_{\alpha'\beta'}(t) \; , \tag{5.18}$$

where

$$\mathcal{M}_{\alpha\beta,\alpha'\beta'} = -\frac{i}{\hbar} (\varepsilon_\alpha - \varepsilon_\beta) \delta_{\alpha\alpha'} \delta_{\beta\beta'} + \mathcal{L}_{\alpha\beta,\alpha'\beta'} \; . \tag{5.19}$$

The first term on the r.h.s. describes the coherent time evolution of the pure system while the second term, $\mathcal{L}$, contains transition rates describing the influence of the dissipative environment [30],

$$\begin{aligned}
\mathcal{L}_{\alpha\beta,\alpha'\beta'} =& \sum_n \left( N_{\alpha\alpha',-n} + N_{\beta\beta',-n} \right) X_{\alpha\alpha',n} X_{\beta'\beta,-n} \\
&- \delta_{\beta\beta'} \sum_{\beta'',n} N_{\beta''\alpha',-n} X_{\alpha\beta'',-n} X_{\beta''\alpha',n} \\
&- \delta_{\alpha\alpha'} \sum_{\alpha'',n} N_{\alpha''\beta',-n} X_{\beta'\alpha'',-n} X_{\alpha''\beta,n} \; .
\end{aligned} \tag{5.20}$$

Here the coefficients are

$$\begin{aligned}
N_{\alpha\beta,n} &= N(\varepsilon_\alpha - \varepsilon_\beta + n\hbar\omega) \; , \\
N(\varepsilon) &= \frac{m\gamma\varepsilon}{\hbar^2} \frac{1}{e^{\varepsilon/k_B T} - 1} \; , \\
X_{\alpha\beta,n} &= \frac{\omega}{2\pi} \int_0^{2\pi/\omega} dt\, e^{in\omega t} \langle \phi_\alpha(t) | \hat{x} | \phi_\beta(t) \rangle \; ,
\end{aligned}$$

where $\gamma$ is the damping rate. Furthermore, steady states are the eigenstates of superoperator $\mathcal{M}$ with zero eigenvalues, since the derivative of a density state is zero, $\dot{\rho} = 0$.

### 5.2.6 Expectation value of $x(t)$

We are interested in calculating the asymptotic expectation value $\langle \hat{x}(t) \rangle$ of the position operator. This is the quantity which can directly be compared to its classical counterpart that is the solution of the classical Duffing equation.

$$\langle \hat{x}(t) \rangle = \text{Tr}\left[\rho(t)\hat{x}\right] = \sum_{\alpha\beta} \rho_{\alpha\beta}(t) X_{\beta\alpha}(t) \ . \tag{5.21}$$

We assume $\langle \hat{x}(t) \rangle \approx A\cos(\omega_{ex}t + \varphi)$, and the amplitude and the phase are given by

$$A = 2\left|\sum_{\alpha\beta} \rho_{\alpha\beta} X_{\beta\alpha,+1}\right| \ , \tag{5.22}$$

$$\begin{aligned}
\varphi = \arctan\left[\frac{\text{Im}\sum_{\alpha\beta}\rho_{\alpha\beta}X_{\beta\alpha,+1}}{\text{Re}\sum_{\alpha\beta}\rho_{\alpha\beta}X_{\beta\alpha,+1}}\right] \\
+ \pi\Theta\left(-\text{Re}\left[\sum_{\alpha\beta}\rho_{\alpha\beta}X_{\beta\alpha,+1}\right]\right)\Theta\left(\text{Im}\left[\sum_{\alpha\beta}\rho_{\alpha\beta}X_{\beta\alpha,+1}\right]\right) \\
- \pi\Theta\left(-\text{Re}\left[\sum_{\alpha\beta}\rho_{\alpha\beta}X_{\beta\alpha,+1}\right]\right)\Theta\left(-\text{Im}\left[\sum_{\alpha\beta}\rho_{\alpha\beta}X_{\beta\alpha,+1}\right]\right) \ ,
\end{aligned} \tag{5.23}$$

where $\Theta$ is the Heaviside function. The range of phase $\varphi$ is from $-\pi$ to $\pi$, but the range of the arctangent funciton is from $-\pi/2$ to $\pi/2$. So, we add Heaviside functions into Eq. (5.23), i.e., the second and the third terms on the right hand side of Eq. (5.23), to extend the range for the phase.

## 5.3 Numerical simulation

We calculate Eq. (5.18) to obtain the time evolution of the density matrix, and obtain the expectation value of the response amplitude using Eq. (5.22). Furthermore, to obtain the steady state, we could ,as a fast method, calculate the eigenvector of superoperator $\mathcal{M}$ in Eq. (5.18) that has a zero eigenvalue, and guarantees $\dot{\rho} = 0$ with

a nontrivial eigenvector. We have also checked the time evolution result of Eq. (5.18) to a long sufficiently final time at which the expectation value of the response value is already stable to make sure the result is the same as the steady-state result obtained from the zero-eigenvalue method.

The mathematical model of a JBA is a quantum Duffing oscillator, Eq. (2.36). Understanding the behavior of a driven quantum Duffing oscillator enables us to understand the behavior of a JBA and understand how to detect the state of a qubit through a readout JBA. An amplitude response curve versus the driving frequency is shown in Fig. 5.1. The shoulder-like curve suggests that a driven JBA has a larger response amplitude state and a smaller response amplitude state corresponding to different ratios of $\omega_{ex}/\omega_0$, respectively, and the JBA transits between these two states when a a slight change of the value of $\omega_{ex}/\omega_0$ is made. Coupled to the JBA, a qubit will change the nature frequency $\omega_0$ of the JBA, and we can use the sensitive property of the JBA transiting between the larger and the smaller response amplitude states to detect the state of the qubit.

## 5.3.1 Amplitude response

A nonlinear oscillator with the nonlinearity coefficient $\alpha$ being zero becomes a harmonic oscillator, of which energy levels' spacings are all the same. This means all multiphoton resonances concentrate at $\omega_{ex}/\omega_0 = 1$. As the nonlinearity coefficient increases, the resonance values of the driving frequency spread out. Additionally, the width of lower N-photon resonances is broader than that of higher ones. In other words, the resonance peak centering on higher driving frequency, which correspond to higher N-photon resonance, is narrower. An amplitude response curve versus the
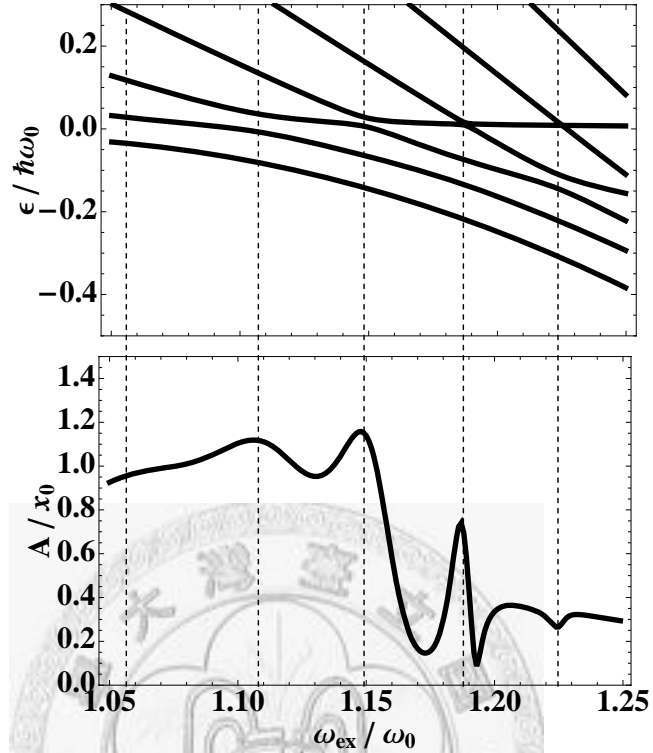
**Figure 5.1** Quasienergy spectrum and response amplitude as a function of the driving frequency. Every avoided crossing in the quasienergy spectrum corresponds to a N-photon excitation. Parameters are $k_B T = 0.1\hbar\omega_0$, $\alpha = 0.1\alpha_0$, $f = 0.1f_0$ and $\gamma = 0.005\omega_0$.

driving frequency is shown in Fig. 5.1, a shoulder-like curve with many peaks at some particular frequency spacings. Each peak corresponds to a certain multiphoton resonance process. Because the resonance values spread out and the amplitude peaks have different widths, at some critical value, for example at $\omega_{ex}/\omega_0 = 1.165$ in Fig. 5.1, the two nearest neighboring peaks do not overlap, creating a very slope curve. In addition, the neighboring peaks at the values less than $\omega_{ex}/\omega_0 = 1.165$ mix, resulting the formation of the high "shoulder" behavior.

The N-photon excitation happens when N-photon's energy, $N\hbar\omega_{ex}$, matches the energy difference between a certain energy level and the ground state. Two quasienergy

levels cross at this point when the driving amplitude vanishes. As driving amplitude increase, the crossing splits more, and the two Floquet states no longer degenerate. Every avoided quasienergy level crossing corresponds to a N-photon excitation.

### 5.3.2 Varying temperatures and the nonlinearity coefficients

Due to fluctuation caused by temperature, the higher the temperature is, the broader the widths of the peaks are. Additionally, the heights of the peaks are suppressed at high temperature. In Fig. 5.2(a), it is obvious that at a hight temperature of $T = T_0$, the shoulder-like shape behavior disappears and the peaks also diminish significantly.

The role of the nonlinearity coefficient $\alpha$ is a little different from others. It controls the anharmonic energy spacings. In other words, it controls the values of the driving frequency for N-photon resonant. The values where the N-photon's energy matches the quasienergy spacing strongly depend on the nonlinearity coefficient. As the value of $\alpha$ increases, every N-photon peak shifts, as shown in Fig. 5.2(b), resulting in the whole curve shift and flatten a little bit toward larger driving frequencies. Moreover, the heights of the peaks decrease for increasing $\alpha$.

### 5.3.3 Varying driving amplitudes

We can expect the N-photon peaks will grow higher and broader with the increase of driving amplitude $f$. In Fig. 5.3(a), we observe that increasing $f$ leads to a shift of the critical point (i.e., the most slope region,) towards larger driving frequencies of the next excitation, which is labeled by the two arrows. Note that the values of the driving frequency for N-photon resonances remain unchanged and just the critical
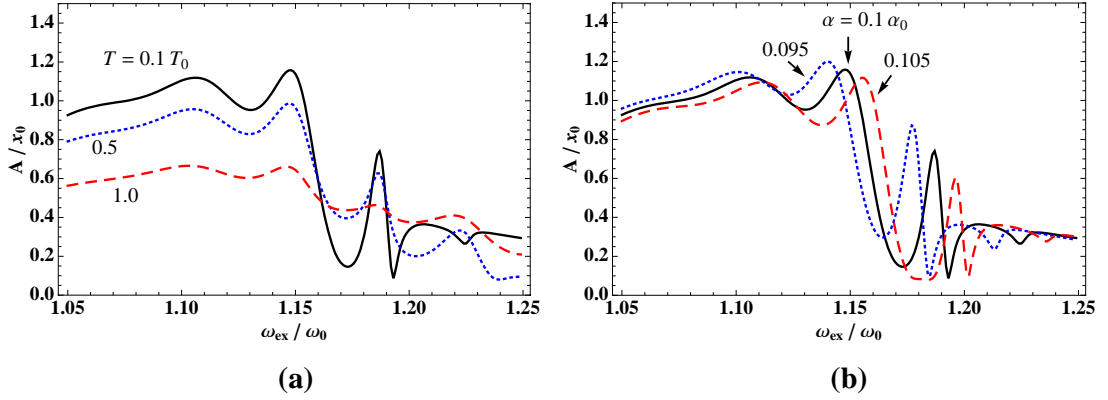
**Figure 5.2** (a)Response amplitude for different values of temperature $T$, $k_B T = 0.1$, 0.5, and $1.0\hbar\omega_0$, with $\alpha = 0.1\alpha_0$. (b)Response amplitude for different value of the nonlinearity $\alpha$, $\alpha = 0.095$, 0.1, and $0.105\alpha_0$ with $k_B T = 0.1\hbar\omega_0$. The remaining parameters are $f = 0.1f_0$ and $\gamma = 0.005\omega_0$.

point moves.

If we fix the driving frequency, we can observe a shoulder-like profile shown in the curve of the response amplitude versus the driving amplitude in Fig. 5.3(b). This behavior is also predicted by classical physics. However, there is no resonance peak appearing and the whole curve is very smooth.

### 5.3.4 Expansion in x space

In the numerical simulations, we write down the Hamiltonian of the anharmonic oscillator in the number basis, $\{|\alpha\rangle\}$, transfer it into the extended Hilbert space $T \otimes R$, then calculate the Floquet states, and finally use the master equation in the basis of the Floquet states to simulate the dynamics of the anharmonic oscillator. After we obtain the results of the simulations, we transfer them back into the extended Hilbert space and then into the number basis. We will represent the results in the position

**(a)**        **(b)**
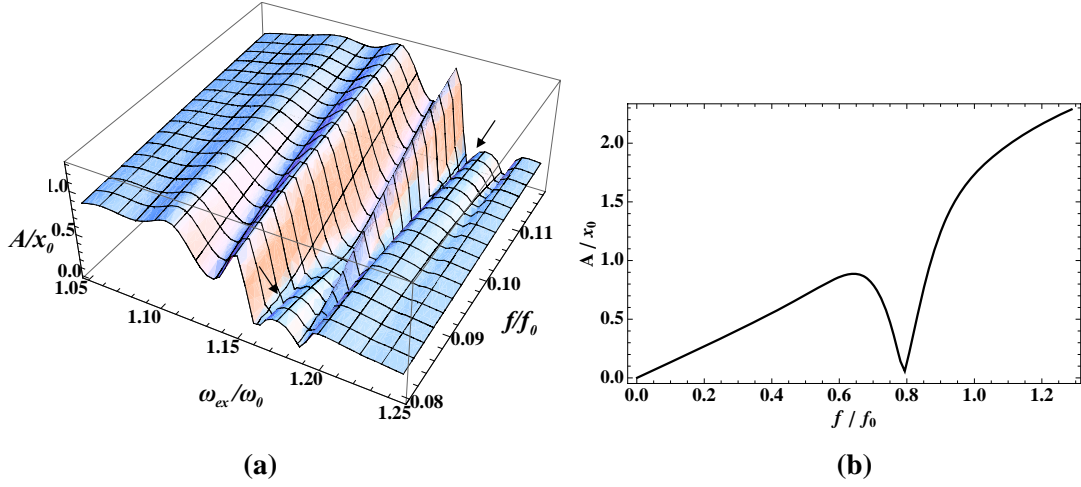
**Figure 5.3** (a) A 3D diagram of the response amplitude versus the driving frequency and the driving amplitude. The two arrows label a shift of the critical area. (b) A response amplitude profile versus the driving amplitude $f$ with $\omega_{ex} = 1.4\omega_0$. The remaining parameters are $k_B T = 0.1\hbar\omega_0$, $\alpha = 0.1\alpha_0$ and $\gamma = 0.005\omega_0$.

space in this subsection. The whole process is as follows,

$$\{|\alpha\rangle\} \Rightarrow \{|\alpha n\rangle\} \rightarrow \{|\phi_\alpha\rangle\} \longrightarrow \{|\phi_\alpha\rangle\} \rightarrow \{|\alpha n\rangle\} \Rightarrow \{|\alpha\rangle\} \rightarrow \{|x\rangle\} \ . \tag{5.24}$$

With Eq. (5.18), we have the dynamics of the density matrix in the Floquet picture. We can calculate the expectation value of the respond amplitude directly in the Floquet picture using Eq. (5.22). However, we try to obtain the dynamics of the desity matrix in the original Hilbert space $R$, and the Fourier expansion of it can be written as

$$\rho(t) = \rho_0 + \rho_1 e^{-i\omega_{ex}t} + \rho_{-1}e^{i\omega_{ex}t} + \rho_2 e^{-i2\omega_{ex}t} + \rho_{-2}e^{i2\omega_{ex}t} + \cdots \ . \tag{5.25}$$

Now we define $2\,|\langle x|\,\rho_1\,|x\rangle|$ as the amplitude distribution function and normalize it to 1. In Fig. 5.4, we observe that there are two peaks in the amplitude distribution function when the driving frequency is near the critical point region. When the driving frequency is away from the critical region, the weights of the two peaks moves from
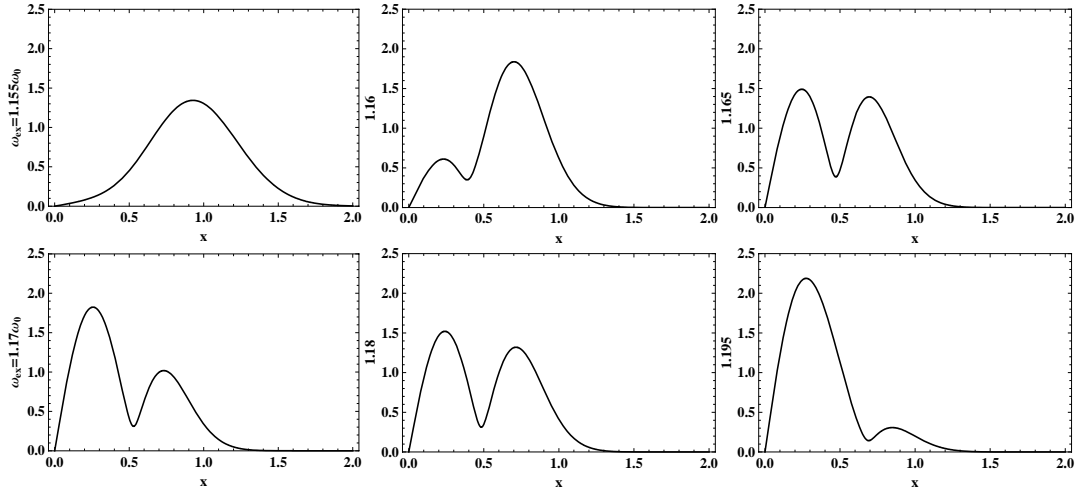
**Figure 5.4** The amplitude distribution function. The two peaks concentrate to one when the driving frequency is away from the critical region. From the upper left to the upper right and then from the lower left to the lower right, $\omega_I = 1.155, 1.16, 1.165, 1.17, 1.18, 1.195\omega_0$. The remaining parameters are $k_B T = 0.1\hbar\omega_0$, $\alpha = 0.1\alpha_0$, $f = 0.1f_0$ and $\gamma = 0.005\omega_0$.

one peak to the other. In classical physics, there are two different stable response amplitude states near the critical point [appendix A]. The two peaks correspond to the two different steady state response amplitudes. We can expect that in the adiabatic condition, with driving frequency increasing from the critical point region toward a smaller value, the oscillator will stay in the large amplitude state with a high probability. On the other hand, when the driving frequency increases from the critical point region to a larger value, the oscillator will mostly stay in the small amplitude state.

# 5.4 Driven quantum Duffing oscillator coupled to a qubit

From Sec. 2.5, we can image a qubit coupled to a readout JBA, whose nature frequency will be effectively shifted depending on the qubit's state. If the driving frequency point of the JBA readout is set in the critical region, Fig. 5.1, the state of the qubit being $|1\rangle$ or $|0\rangle$ will move the value of $\omega_{ex}/\omega_0$ to the left or the right, respectively, and the expectation value of the stable response amplitude will change significantly.

We define the Hamiltonian of the system as,

$$
\begin{aligned}
H &= H_q + H_I + H_J \\
&= \hbar\omega_q \sigma_z \otimes \hat{I}_J + \hbar\omega_I \sigma_z \otimes \hat{n} + \hat{I}_q \otimes \left( \hbar\omega_J \hat{n} + \frac{\alpha}{4}\hat{x}^4 + \hat{x} f \cos(\omega_{ex} t) \right) ,
\end{aligned}
\tag{5.26}
$$

where $\omega_q$, $\omega_J$, and $\omega_I$ are the nature frequency of the qubit, the nature frequency of the JBA oscillator, and the coupling strength, respectively, $\hat{I}_J$ and $\hat{I}_q$ are identity of the JBA's Hilbert space and that of the qubit's, respectively, and $\hat{n} = \hat{a}^+ \hat{a}$ is the number operator of the JBA oscillator.

## 5.4.1 The JBA response

Being coupled to a qubit, the readout JBA oscillator at a fixed driving force and a fixed driving frequency shows different response amplitudes depending on the state of the qubit. It is shown in Fig. 5.5(a) that the larger response amplitude state corresponds to the qubit's state being $|1\rangle$, while the lower amplitude state corresponds to the qubit being in $|0\rangle$ state. The distribution functions with the qubit's state being $|0\rangle$ (dotted line) or $|1\rangle$ (solid line) for different values of the coupling strength $\omega_I$ are shown in

Figs. 5.5(c)(d) and (e). As shown in 5.5(d) for $\omega_I = 0.024\omega_0$, when the qubit's state is $|1\rangle$, most of the distribution function stay in the large $x$ regime, but little stay in the small $x$ regime. The situation for $|0\rangle$ state is however the opposite. Intrinsic errors in the amplitude distribution function have been found in experiment [22]. In experiment, for a qubit being in $|0\rangle$ (or $|1\rangle$), there is a nonvanishing probability of finding the JBA oscillator in the large (small) amplitude state. This intrinsic error may be understood from the amplitude distribution function shown in Figs. 5.5(c)(d) and (e). For a small coupling strength $\omega_I$, it is hard to read out the qubit state from the JBA oscillator amplitude as the distribution function has significant weights in both the small and large amplitude regimes (see Fig. 5.5(c)). On the other hand, when the coupling strength is large, the weight of the distribution function moves toward to the small $x$ regime for qubit state being $|0\rangle$ and to the large $x$ regime for qubit state being $|1\rangle$. However, the larger coupling strength also causes the broadening of the distribution functions, resulting in an overlap of the distribution functions that correponds to two qubit states.

## 5.4.2 Behaviors of the qubit

In this subsection, we discuss behaviors of the qubit in two situations. First, the Hamiltonian of the qubit has not only the $\sigma_z$ term but also an additional $\sigma_x$ term. This may be caused by the qubit's or the coupling's flaw. In the case, the non-demonlition condition is not fullfilled [23]. Second, the qubit is coupled to an environment so that it may decohere or relax even without the presence of the JBA readout device.

Even if there is no other environment coupled to the qubit, the JBA readout device still cause the qubit dephasing because of the $\sigma_z$ coupling to the qubit. If the Hamiltonian of the qubit is not exactly $\hbar\omega_q\sigma_z$ but $\hbar\omega_q\sigma_z + \hbar\omega_{qx}\sigma_x$, the steady-state
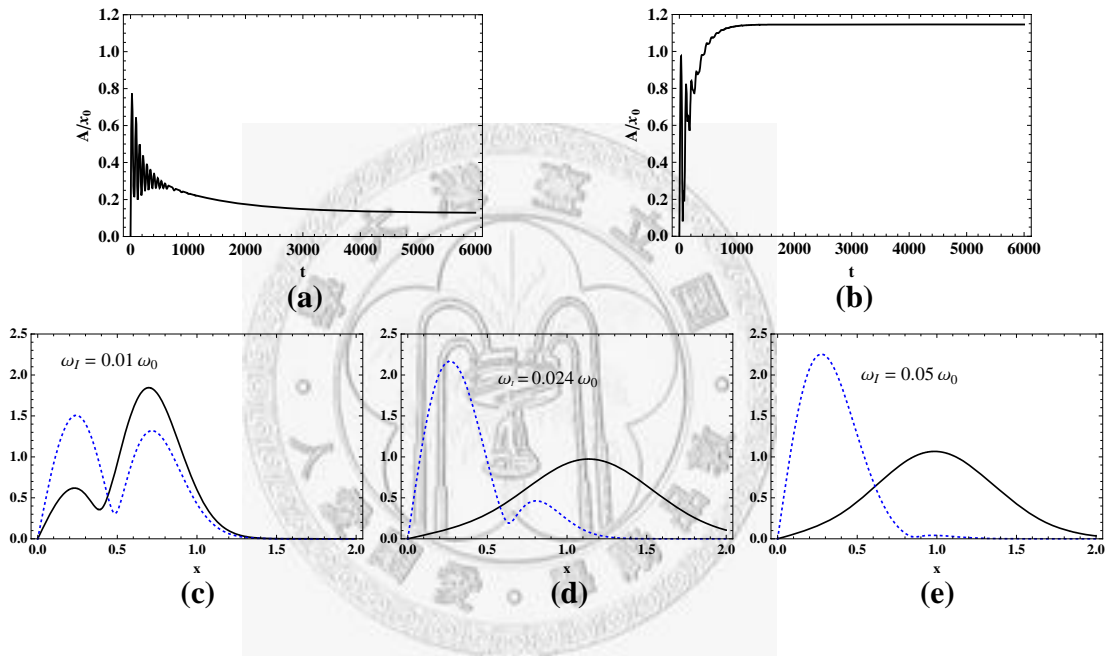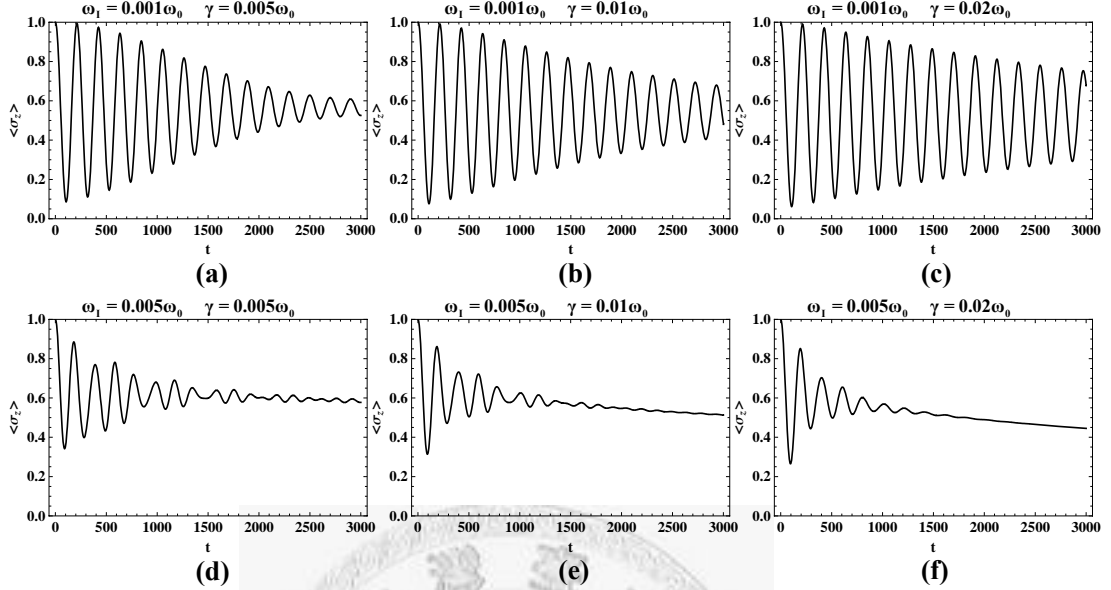
**Figure 5.5** The time evolution diagrams of the response amplitude when qubit's states are (a) $|0\rangle$ and (b) $|1\rangle$ with $\omega_I = 0.024$. (c)(d)(e) The amplitude distribution function with qubit's state $|0\rangle$ (dotted line) or $|1\rangle$ (solid line). The driving frequency $\omega_{ex}$ equals $1.17\omega_0$. The remaining parameters are $k_B T = 0.1\hbar\omega_0$, $\alpha = 0.1\alpha_0$, $f = 0.1f_0$ and $\gamma = 0.005\omega_0$.

expectation value of $\sigma_z$ will no longer in $+1$ or $-1$ as the $\sigma_x$ term will move the stationary state value away from that value. If $\omega_I \gg \omega_{qx}$ the steady-state $\langle \sigma_z \rangle$ will stay in $+1$ if the initial qubit state is $|1\rangle$. If $\omega_I < \omega_{qx}$, the steady state of $\langle \sigma_z \rangle$ will move away from $+1$, depending also on the value of $\omega_q$. Furthermore, the oscillation is not very regular, and we can observe some "sudden veers" in Fig. 5.6(d). The JBA's environment fluctuates the JBA and influences the qubit through the JBA. We can expect if the coupling strength $\omega_I$ is larger, which results in strong influence of the JBA on the qubit, decoherence rate of the qubit is larger. The influence of the damping rate $\gamma$ of the JBA oscillator on the qubit dynamics is a little bit subtle. One may expect the larger value of $\gamma$ (stronger environment influence on JBA) may result in a larger decohere on the qubit as shown in Figs. 5.6(d)(e) and (f). However, when the coupling strength is small, if the value of $\gamma$ is increased, the decoherence rate of the qubit is small instead as shown in Fig. 5.6(a)(b) and (c). This may be because the JBA is damped to its steady state so fast that the influence on the qubit becomes small.

Next, we assume an environment is coupled to the qubit through a $\sigma_x$ coupling term. For this purpose, we need to add another dissipative term $\mathcal{L}'_{\alpha\beta,\alpha'\beta'}$ to Eq. (5.19),

$$
\begin{aligned}
\mathcal{L}'_{\alpha\beta,\alpha'\beta'} = &\sum_n \left( N'_{\alpha\alpha',-n} + N'_{\beta\beta',-n} \right) \Sigma_{\alpha\alpha',n}\Sigma_{\beta'\beta,-n} \\
&- \delta_{\beta\beta'} \sum_{\beta'',n} N'_{\beta''\alpha',-n}\Sigma_{\alpha\beta'',-n}\Sigma_{\beta''\alpha',n} \\
&- \delta_{\alpha\alpha'} \sum_{\alpha'',n} N'_{\alpha''\beta',-n}\Sigma_{\beta'\alpha'',-n}\Sigma_{\alpha''\beta,n} \ ,
\end{aligned}
\tag{5.27}
$$

**Figure 5.6** The $\sigma_z$ expectation value of the qubit. The JBA's environment influences the qubit through the JBA. The remaining parameters are $\omega_q = 0.01\omega_0$, $\omega_{qx} = 0.01$, $\omega_{ex} = 1.16$, $k_B T = 0.1\hbar\omega_0$, $\alpha = 0.1\alpha_0$, $f = 0.1f_0$. The initial state of the qubit is $|1\rangle$.

where

$$N'_{\alpha\beta,n} = N' \left( \varepsilon_\alpha - \varepsilon_\beta + n\hbar\omega \right) ,$$

$$N' \left( \varepsilon \right) = \frac{\gamma_q \varepsilon}{\hbar^2} \frac{1}{e^{\varepsilon/k_B T} - 1} ,$$

$$\Sigma_{\alpha\beta,n} = \frac{\omega}{2\pi} \int_0^{2\pi/\omega} dt e^{in\omega t} \langle \phi_\alpha \left( t \right) | \sigma_x \otimes I_J | \phi_\beta \left( t \right) \rangle ,$$

Where the relaxation rate $\gamma_q$ determines the decay rate of the qubit. If the relaxation rate is very large, the JBA could not reflect the qubit's state and would not reach the response amplitude value that it is supposed to reach before the qubit relaxes. In contrast, if the relaxation rate is small, the JBA can read out the information of the qubit state before the qubit relaxes. The time evolution of the expectation value of the response amplitude and the distribution functions in the presence of the qubit relaxation are shown in Fig. 5.7. The expectation value decays with time and
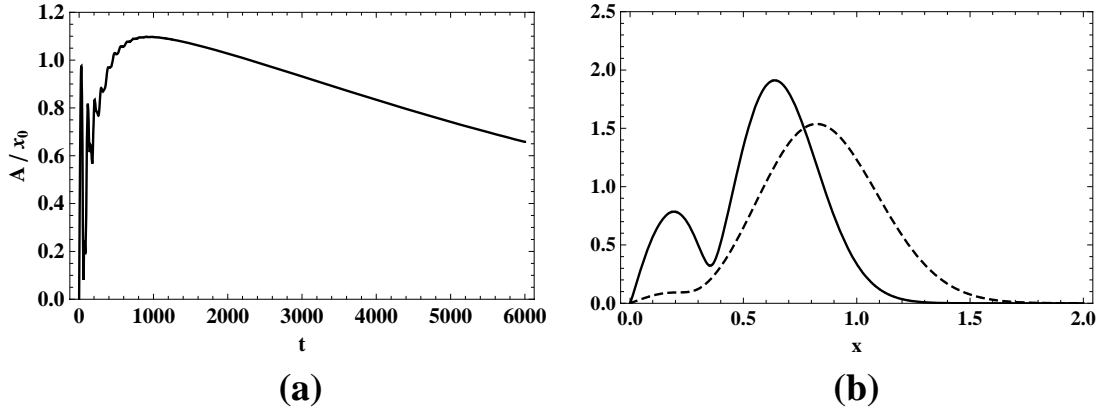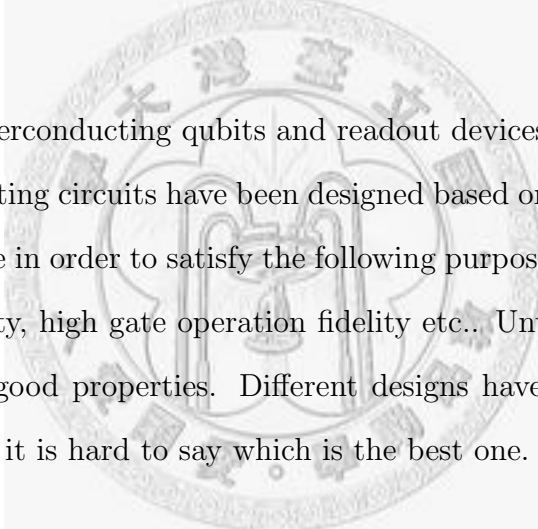
**Figure 5.7** (a) The amplitude response. The qubit decays from $|1\rangle$ to $|0\rangle$ caused by its environment, which making the response amplitude can't maintain a higher level. (b) The amplitude distribution function. Solid line: t=6000. Dashed line: t=4000. $\gamma = 0.005$, $\gamma_q = 0.0002$, $\omega_q = 0.1$, and $\omega_I = 0.024$.

the response amplitude can't maintain at a large value. In addition, the distribution function changing from a single peak centering at a large $x$ value at $t = 4000$ to a two-peak structure at $t = 6000$ in which the peak centering at a small $x$ value gains considerable weight in small $x$ regime.

# Chapter 6

# Conclusions

Many kinds of superconducting qubits and readout devices have been proposed, and many superconducting circuits have been designed based on these qubits and devices. All these efforts are in order to satisfy the following purposes: high coherence quality, high readout fidelity, high gate operation fidelity etc.. Until now, no one design can fulfill all of these good properties. Different designs have different advantages and disadvantages. So, it is hard to say which is the best one.

In this thesis, we have described briefly three kinds of qubits and concentrated on a quantronium coupled to a Josephson bifurcation amplifier (JBA) as the readout device. The shift of the resonance frequency of the JBA depends on the state of the measured qubit. As a result, the amplitude response of the JBA reveals the state of the measured qubit. During the measurement process, the JBA remains in zero-voltage state, which avoids the dissipation problem caused by voltage switching to the normal state in other Josephson junction readout schemes.

For the purpose of simulating a driven JBA, we have investigated the Floquet for-

malism, which is a good tool to deal with a time-periodic problem. The Floquet formalism transfers a time-dependent problem in a Hilbert space to a time-independent problem in an extended Hilbert space. We can truncate the Floquet Hamiltonian based on the strength of the driving amplitude and the final time of the evolution. Furthermore, the quasienergy spectrum provides a good picture of muti-photon excitation processes.

We have also studied the Born-Markovian master equation of a driven system. We find that the difficulty caused by the time-ordering operator, which appears when a driving force is added to the system, can be overcome by using the Floquet states as the basis. The combination of the Born-Markovian master equation and the Floquet states is so-called the Floquet-Born-Markovian master equation.

Finally, we have discussed the behavior of a JBA, whose mathematical model is a driven quantum Duffing oscillator. We have also presented the dynamical properties of a JBA coupled to a qubit. A shoulder-like shape in the amplitude response versus the driving frequency plot is presented accompany with quasienergy spectrum of multiphoton excitations. We have simulated the measurement process that when a JBA is coupled to a qubit, the amplitude response of the JBA will evolve to a higher level or a lower level depending on the state of the qubit. We have also discussed the dynamics of a qubit subjected to a measurement by a JBA and also coupled to an extra environment. If the coupling between the qubit and the JBA is much small, when the damping constant of the JBA's environment is larger, the influence on the qubit is instead smaller.

Overall, the JBA is a very good readout device for superconducting qubit as it will

not induce dissipation as other voltage switching readout devices do. However, some possible measurement related errors of the devices, discussed in this thesis, should be overcome or avoided in order to improve the readout fidelity of the device.

# Bibliography

[1] P. W. Shor, "Algorithms for quantum computation: discrete logarithms and factoring," In 35th Annual Symposium on Foundations of Computer Science. IEEE Press, Los Alamos (1994).

[2] P. W. Shor, "Polynomial-time algorithms for prime factorization and discrete logarithms on a quantum computer," SIAM J. Computing 26 (1997).

[3] L. K. Grover, "A fast quantum mechanical algorithm for database search," In *STOC '96: Proceedings of the twenty-eighth annual ACM symposium on Theory of computing*, pp. 212–219 (ACM, New York, NY, USA, 1996).

[4] L. K. Grover, "Quantum Mechanics Helps in Searching for a Needle in a Haystack," Phys. Rev. Lett. **79,** 325–328 (1997).

[5] L. K. Grover, "Quantum Computers Can Search Rapidly by Using Almost Any Transformation," Phys. Rev. Lett. **80,** 4329–4332 (1998).

[6] M. A. Nielsen and I. L. Chuang, *Quantum Computation and Quantum Information*, 2 ed. (Cambridge University Press, 2001).

[7] I. Siddiqi, R. Vijay, F. Pierre, C. M. Wilson, M. Metcalfe, C. Rigetti, L. Frunzio, and M. H. Devoret, "RF-Driven Josephson Bifurcation Amplifier for Quantum Measurement," Physical Review Letters **93,** 207002+ (2004).

[8] M. I. Dykman and M. A. Krivoglaz, "Fluctuations in nonlinear systems near bifurcations corresponding to the appearance of new stable states," Physica A **104,** 480 (1980).

[9] V. E. Manucharyan, E. Boaknin, M. Metcalfe, R. Vijay, I. Siddiqi, and M. Devoret, "Microwave bifurcation of a Josephson junction: Embedding-circuit requirements," Physical Review B (Condensed Matter and Materials Physics) **76,** 014524 (2007).

[10] J. Clarke and F. K. Wilhelm, "Superconducting quantum bits," Nature **453,** 1031–1042 (2008).

[11] J. Q. You and F. Nori, "Superconducting Circuits and Quantum Information," Physics Today **58,** 42–47 (2005).

[12] G. Wendin and V. S. Shumeiko, "Superconducting Quantum Circuits, Qubits and Computing," arxiv:cond-mat (2005).

[13] Y. Makhlin, G. Schon, and A. Shnirman, "Quantum-state engineering with Josephson-junction devices," Reviews of Modern Physics **73,** 357+ (2001).

[14] M. H. Devoret, A. Wallraff, and J. M. Martinis, "Superconducting Qubits: A Short Review," arxiv:cond-mat (2004).

[15] C. Kittel, *Introduction to Solid State Physics*, 8 ed. (John Wiley and Sons (WIE), 2004).

[16] M. Tinkham, *Introduction to Superconductivity: Second Edition (Dover Books on Physics)*, 2 ed. (Dover Publications, 2004).

[17] J. Koch, T. M. Yu, J. Gambetta, A. A. Houck, D. I. Schuster, J. Majer, A. Blais, M. H. Devoret, S. M. Girvin, and R. J. Schoelkopf, "Charge-insensitive

qubit design derived from the Cooper pair box," Physical Review A **76,** 042319 (2007).

[18] J. E. Mooij, T. P. Orlando, L. Levitov, L. Tian, C. H. v. d. Wal, and S. Lloyd, "Josephson Persistent-Current Qubit," Science **285,** 1036–1039 (1999).

[19] D. Vion, A. Aassime, A. Cottet, P. Joyez, H. Pothier, C. Urbina, D. Esteve, and M. H. Devoret, "Manipulating the Quantum State of an Electrical Circuit," Science **296,** 886–889 (2002).

[20] G. Ithier *et al.*, "Decoherence in a superconducting quantum bit circuit," Physical Review B **72,** 134519 (2005).

[21] I. Siddiqi, R. Vijay, M. Metcalfe, E. Boaknin, L. Frunzio, R. J. Schoelkopf, and M. H. Devoret, "Dispersive measurements of superconducting qubit coherence with a fast latching readout," Physical Review B **73,** 054510 (2006).

[22] N. Boulant *et al.*, "Quantum nondemolition readout using a Josephson bifurcation amplifier," Physical Review B **76,** 014525 (2007).

[23] A. Lupascu, C. J. M. Verwijs, R. N. Schouten, C. J. P. M. Harmans, and J. E. Mooij, "Nondestructive readout for a superconducting flux qubit," Physical Review Letters **93,** 177006 (2004).

[24] J. H. Shirley, "Solution of the Schrödinger Equation with a Hamiltonian Periodic in Time," Physical Review **138,** B979+ (1965).

[25] A. G. Fainshtein, N. L. Manakov, and L. P. Rapoport, "Some general properties of quasi-energetic spectra of quantum systems in classical monochromatic fields," Journal of Physics B **11,** 2561 (1978).

[26] S.-I. Chu and D. A. Telnov, "Beyond the Floquet theorem: generalized Floquet formalisms and quasienergy methods for atomic and molecular multiphoton processes in intense laser fields," Physics Reports **390,** 1–131 (2004).

[27] S. Kohler, T. Dittrich, and P. Hänggi, "Floquet-Markovian description of the parametrically driven, dissipative harmonic quantum oscillator," Physics Review E **55,** 300–313 (1997).

[28] S. Kohler, R. Utemann, and P. Hänggi, "Coherent and incoherent chaotic tunneling near singlet-doublet crossings," Physics Review E **58,** 7219–7230 (1998).

[29] M. Thorwart, P. Reimann, P. Jung, and R. F. Fox, "Quantum hysteresis and resonant tunneling in bistable systems," Chemical Physics **235,** 61–80 (1998).

[30] V. Peano and M. Thorwart, "Dynamics of the quantum Duffing oscillator in the driving induced bistable regime," Chemical Physics **322,** 135–143 (2006).

# Appendix A

# Classical Duffing oscillation

There are many methods for obtaining approximated solutions of nonlinear oscillator systems in different situations. Those methods can be found in most non-linear physics text books. In this chapter we take a short review of a useful technique for obtaining approximated periodic in time solutions of second-order differential equations with weak nonlinearity and subject to a harmonic forcing term.

Now we consider an equation of motion of a forced nonlinear oscillator,

$$\ddot{x} + k\dot{x} + \omega_0^2 \sin x = F \cos \omega t \ . \tag{A.1}$$

With the assumption of small nonlinearity

$$\sin x \approx x - \frac{1}{6}x^3 \ , \tag{A.2}$$

Eq. (A.1) becomes, approximately,

$$\ddot{x} + k\dot{x} + \omega_0^2 x - \frac{1}{6}\omega_0^2 x^3 = F \cos \omega t \ . \tag{A.3}$$

Let us define some notations for convenience,

$$\tau = \omega t, \quad \Omega^2 = \omega_0^2/\omega^2, \quad ,\varepsilon_0 = \frac{1}{6}\Omega^2, \quad K = k/\omega, \quad \Gamma = F/\omega^2 \ . \tag{A.4}$$

We have

$$x'' + Kx' + \Omega^2 x - \varepsilon_0 x^3 = \Gamma \cos \tau \, , \tag{A.5}$$

where the primes symbol and double prime symbol are used to represent differentiation with respect to $\tau$. We also assume that $\Gamma$, $K$ and $\Omega^2 - 1$ are very small,

$$\Gamma = \varepsilon_0 \gamma, \quad K = \varepsilon_0 \kappa \quad , \Omega^2 = 1 + \varepsilon_0/\beta \quad (\gamma, \kappa > 0) \, , \tag{A.6}$$

which corresponds to weak excitation, small damping and near-resonance of the linearized equation, respectively. Eq. (A.5) becomes

$$x'' + x = \varepsilon_0 \left( \gamma \cos \tau - \kappa x' - \beta x + x^3 \right) \, . \tag{A.7}$$

Here we introduce the perturbation method, which is similar to the time-independent perturbation theory in quantum mechanics. We consider the family of differential equations

$$x'' + x = \varepsilon \left( \gamma \cos \tau - \kappa x' - \beta x + x^3 \right) \, , \tag{A.8}$$

where $\varepsilon$ is a parameter in an interval $I_\epsilon$ which includes $\varepsilon = 0$. When $\varepsilon = \varepsilon_0$, we recover Eq. (A.7). Consequently, the solutions will be the functions of both $\tau$ and $\varepsilon$, and the solutions may be represented in the form of a power series in $\varepsilon$,

$$x(\varepsilon, \tau) = x_0(\tau) + \varepsilon x_1(\tau) + \varepsilon^2 x_2(\tau) + \dots \, . \tag{A.9}$$

We shall be concerned only with periodic solutions having the period, $2\pi$, of the forcing term, which means that

$$x_i(\tau + 2\pi) = x_i(\tau), \quad i = 0, 1, 2, \dots \, . \tag{A.10}$$

Substituting Eq. (A.9) into Eq. (A.8), we obtain, based on the balance of the

coefficients of the resultant equation for each power $\varepsilon$,

$$x_0'' + x_0 = 0 \ , \tag{A.11}$$

$$x_1'' + x_1 = \gamma \cos \tau - \kappa x_0' - \beta x_0 + x_0^3 \ , \tag{A.12}$$

$$x_2'' + x_2 = -\kappa x_1' - \beta x_1 + 3x_0^2 x_1 \ , \tag{A.13}$$

and so on.

The solution of Eq. (A.11) is

$$x_0(\tau) = a_0 \cos \tau + b_0 \sin \tau \ . \tag{A.14}$$

Now substituting Eq. (A.14) into Eq. (A.12), we have

$$\begin{aligned} x_1'' + x_1 = & \left\{ \gamma - \kappa b_0 + a_0 \left[ -\beta + \frac{3}{4} \left( a_0^2 + b_0^2 \right) \right] \right\} \cos \tau \\ & + \left\{ \kappa a_0 + b_0 \left[ -\beta + \frac{3}{4} \left( a_0^2 + b_0^2 \right) \right] \right\} \sin \tau \\ & + \frac{1}{4} a_0 \left( a_0^2 - 3b_0^2 \right) \cos 3\tau + \frac{1}{4} b_0 \left( 3a_0^2 - b_0^2 \right) \sin 3\tau \ . \end{aligned} \tag{A.15}$$

Since $\cos \tau$ and $\sin \tau$ terms in Eq. (A.15) will make the solution of $x_1$ have the form of $\tau \cos \tau$ or $\tau \sin \tau$ but we concern only the solution of $x_1$ that has a period $2\pi$, the coefficients of $\cos \tau$ and $\sin \tau$ terms should be zero,

$$\kappa a_0 - b_0 \left\{ \beta - \frac{3}{4} \left( a_0^2 + b_0^2 \right) \right\} = 0 \ , \tag{A.16}$$

$$\kappa b_0 + a_0 \left\{ \beta - \frac{3}{4} \left( a_0^2 + b_0^2 \right) \right\} = \gamma \ . \tag{A.17}$$

We define $r_0$ as the amplitude of the generating solution,

$$r_0 = \sqrt{\left( a_0^2 + b_0^2 \right)} > 0 \ . \tag{A.18}$$

By squaring and adding Eq. (A.16) and Eq. (A.17), we obtain the following equation for $r_0^2$,

$$r_0^2 \left\{ \kappa^2 + \left( \beta - \frac{3}{4} r_0^2 \right)^2 \right\} = \gamma^2 \ . \tag{A.19}$$

After $r_0$ is solved, $a_0$ and $b_0$ can be also solved from Eq. (A.16) and Eq. (A.17). Then, putting $a_0$ and $b_0$, which make the coefficients of $\cos\tau$ and $\sin\tau$ zero, back into Eq. (A.15), we have

$$x_1'' + x_1 = \frac{1}{4}a_0\left(a_0^2 - 3b_0^2\right)\cos 3\tau + \frac{1}{4}b_0\left(3a_0^2 - b_0^2\right)\sin 3\tau , \qquad (A.20)$$

and the solution is

$$x_1(\tau) = a_1\cos\tau + b_1\sin\tau - \frac{1}{32}a_0\left(a_0^2 - 3b_0^2\right)\cos 3\tau - \frac{1}{32}b_0\left(3a_0^2 - b_0^2\right)\sin 3\tau . \quad (A.21)$$

If higher order solutions are needed, we can repeat the same steps to get the solutions of $x_2$, $x_3$, $x_4$ and so on. Besides, all equations to determine $a_i$ and $b_i$ are linear equations. That makes the process much less complicated.

Let us go back to the amplitude equation Eq. (A.19) and translate it into the parameters of Eq. (A.1). We have

$$r_0^2\left\{k^2\omega^2 + \left(\omega^2 - \omega_0^2 + \frac{1}{8}\omega_0^2 r_0^2\right)^2\right\} = F^2 , \qquad (A.22)$$

where $r_0$ must be bigger than zero. The solution for $\omega^2$ is

$$\omega^2 = \frac{1}{2}\left\{2\omega_0^2\left(1 - \frac{1}{8}r_0^2\right) - k^2 \pm \sqrt{k^4 - 4\omega_0^2 k^2\left(1 - \frac{1}{8}r_0^2\right) + 4F^2/r_0^2}\right\} . \qquad (A.23)$$

The response amplitude $r_0$ as a function of the driving frequency is shown in Fig. A.1. When the driving amplitude $F$ approach to zero, the response curve is similar to a linear response curve. The bigger the driving amplitude $F$ is, the more seriously the response curve bends over, as shown in Fig. A.1(b). If $F$ is smaller than a critical value, the response curve is a single value function. If $F$ is beyond the critical value, the oscillator could have three alternative forced responses, two stable responses and one metastable response, shown in Fig. A.1, constituting a
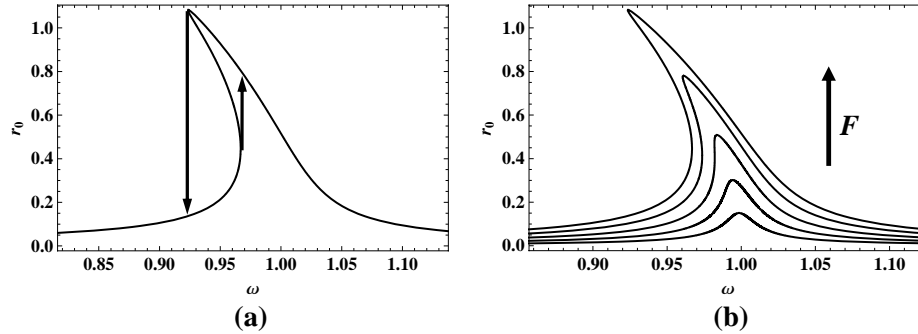
**Figure A.1** The response amplitude profile. (a)The arrows indicate where the response amplitude must jump up to a bigger or a lower response amplitude. $\omega_0 = 1$, $k = 0.02$ and $F = 0.02$ (b)The response curve is for different values of the driving amplitude strength. $\omega_0 = 1$, $k = 0.02$ and, from the bottom to the top, $F = 0.003$, $0.006$, $0.01$, $0.015$ and $0.02$.
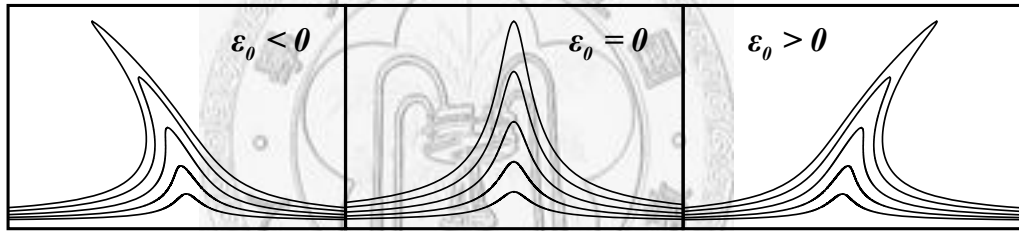


**Figure A.2** $\epsilon_0$ determines the direction of the response amplitude's turning

jump phenomenon. Choosing a fixed $F$ which is bigger than the critical value, we increase driving frequency $\omega$ from some value much smaller than $\omega_0$. When the driving frequency reaches the reverse point, there is no continue solution and the response amplitude must jump up to a bigger response amplitude as indicated in Fig. A.1(a). Now we consider another situation that we decrease the driving frequency from the other side. When the response amplitude climbs up to the summit, it can't descend flatly and must "drop" suddenly to a lower value as shown in Fig. A.1(a). Note that the reverse point in the first situation and the summit in the second situation correspond respectively to different driving frequency values.

Now we consider a more general case,

$$\ddot{x} + k\dot{x} + \omega_0^2 x + \epsilon_0 x^3 = F\cos\omega t \ , \tag{A.24}$$

where $\epsilon_0$ is independent to $\omega_0$. We set $\omega_0 = 1$ for convenience. Using the perturbative method we mentioned before, we have the amplitude response equation,

$$r_0^2 \left\{ k^2 \omega^2 + \left( \omega^2 - 1 - \frac{3}{4}\epsilon_0 r_0^2 \right)^2 \right\} = F^2 \ . \tag{A.25}$$

The nature of the response diagrams in the case of $\epsilon_0 < 0$, $\epsilon_0 = 0$, and $\epsilon_0 > 0$ is shown in Fig. A.2. The response curves bend over to different sides depending on the sign of $\epsilon_0$.